

**DOKUZ EYLÜL UNIVERSITY**  
**GRADUATE SCHOOL OF NATURAL AND APPLIED SCIENCES**

**ESTIMATION OF TRAFFIC DENSITY BASED  
ON PAST DENSITY INFORMATION FOR  
ADAPTIVE TRAFFIC MANAGEMENT**



**by**

**Fevzi Yasin KABABULUT**

**September, 2015**

**İZMİR**

**ESTIMATION OF TRAFFIC DENSITY BASED  
ON PAST DENSITY INFORMATION FOR  
ADAPTIVE TRAFFIC MANAGEMENT**

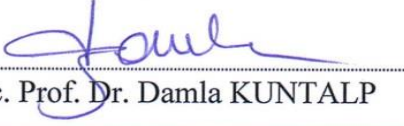
**A Thesis Submitted to the  
Graduate School of Natural and Applied Sciences of Dokuz Eylül University  
In Partial Fulfillment of the Requirements for the Degree of Master of  
Science in Electrical and Electronics Engineering**

**by  
Fevzi Yasin KABABULUT**

**September, 2015  
İZMİR**


## M.Sc THESIS EXAMINATION RESULT FORM

We have read the thesis entitled “ESTIMATION OF TRAFFIC DENSITY BASED ON PAST DENSITY INFORMATION FOR ADAPTIVE TRAFFIC MANAGEMENT” completed by FEVZİ YASIN KABABULUT under supervision of ASSOC. PROF. DR. DAMLA KUNTALP and we certify that in our opinion it is fully adequate, in scope and in quality, as a thesis for the degree of Master of Science.




Assoc. Prof. Dr. Damla KUNTALP

Supervisor

  
Assoc. Prof. Dr. Olcay Akay

(Jury Member)

  
Asst. Prof. Dr. Mehmet Yılmaz

(Jury Member)

  
Prof. Dr. Ayşe OKUR

Director

Graduate School of Natural and Applied Sciences

## ACKNOWLEDGEMENT

Firstly I am very grateful to my life partner and wife Ebru Kababulut for her support and encouragement during my graduate education and especially for her help in writing this thesis.

Undoubtedly the biggest contributions in making this thesis belong to my advisor Assoc. Prof. Dr. Damla Kuntalp and Dokuz Eylul University assistant and PhD student Timur Düzenli. For her valuable review, guidance, and contribution I am very grateful to my advisor Assoc. Prof. Dr. Damla Kuntalp. I am indebted to Timur Düzenli for sharing all kinds of information and his valuable opinions with me. I would like to thank Assoc. Prof. Dr. Olcay Akay and all members of the Dokuz Eylul University Electrical and Electronics Faculty who have supported me at courses and other times.

I would like to thank Hakan Dönmez, Özkan Dönmez, and Muhammed Alyürük because of their contribution to traffic data for my thesis. I also would like to thank my best friend Adem Kara and Ufuk Ali Arslan for their help in writing this thesis and other Transport, Maritime Affairs and Communications Ministry III. Regional Directorate employees especially Hilmi Koç for their support during my graduate education.

Finally, of course, I am indebted to all my family members especially my mother and my father for always believing in me and for their support.

Fevzi Yasin KABABULUT

# **ESTIMATION OF TRAFFIC DENSITY BASED ON PAST DENSITY INFORMATION FOR ADAPTIVE TRAFFIC MANAGEMENT**

## **ABSTRACT**

Traffic congestion which causes economic, environmental and even individual psychological troubles not only in Turkey but all over the world, is a very serious problem. Developed intelligent traffic systems in recent years aim to produce solutions to this problem by monitoring the traffic and applying adaptive decision strategies based on estimations about the future situations. The core problem of these systems consists of the estimation of traffic density reliably.

In the literature part of the thesis we will summarize the most commonly used density estimation methods. In the application part of the thesis we will examine four different algorithms proposed for traffic density estimation which are inspired by the methods used to estimate the spectral holes in cognitive radio applications. Data used in this study is received from Istanbul Traffic Control Center and has been converted into ternary and binary versions depending on the average speed of the traffic flow. In the proposed algorithms, density state at the 60th minute of the considered road is estimated by looking at the past 50 minutes of density data of the same road or adjacent two roads. Different simulations have been performed using these algorithms and results are evaluated based on several performance criteria.

**Keywords:** Density estimation, traffic, congestion, cognitive radio

# ADAPTİF TRAFİK YÖNETİMİ İÇİN GEÇMİŞ YOĞUNLUK BİLGİLERİNE DAYALI TRAFİK YOĞUNLUĞU TAHMİNİ

## ÖZ

Sadece Türkiye’de değil tüm dünyada ekonomik, çevresel ve hatta bireysel psikolojik sorunlara yol açan trafik sıkışıklığı, çok ciddi bir problemdir. Son yıllarda geliştirilen akıllı trafik sistemleri, trafiği izleyerek ve gelecek durumlar hakkındaki tahminlere dayanan adaptif karar stratejilerini uygulayarak bu soruna çözüm üretmeyi hedeflemektedir. Bu sistemlerin temel problemini güvenilir trafik yoğunluğu tahmini oluşturur.

Tezin literatür bölümünde en sık kullanılan yoğunluk tahmin yöntemlerini özetleyeceğiz. Tezin uygulama kısmında ise bilişsel radyo uygulamalarında spektral boşlukları tahmin etmek için kullanılan yöntemlerden esinlenen trafik yoğunluğu tahmini için önerilen dört farklı algoritmayı inceleyeceğiz. Bu çalışmada kullanılan veriler İstanbul Trafik Kontrol Merkezi'nden alınmıştır ve trafik akışının ortalama hızına bağlı olarak üçlü ve ikili versiyonlara çevrilmiştir. Önerilen algoritmalarda, dikkate alınan yolun 60. dakikadaki yoğunluk durumu, aynı yolun ya da bitişik iki yolun geçmiş 50 dakikadaki yoğunluk verilerine bakarak tahmin edilmektedir. Bu algoritmaları kullanarak farklı simülasyonlar gerçekleştirilmiştir ve sonuçlar çeşitli performans kriterlerine göre değerlendirilmiştir.

**Anahtar kelimeler:** Yoğunluk tahmini, trafik, sıkışıklık, bilişsel radyo

## CONTENTS

	<b>Page</b>
M.Sc THESIS EXAMINATION RESULT FORM .....	ii
ACKNOWLEDGEMENT .....	iii
ABSTRACT .....	iv
ÖZ .....	v
LIST OF FIGURES .....	viii
LIST OF TABLES .....	ix
<b>CHAPTER ONE-INTRODUCTION .....</b>	<b>1</b>
<b>CHAPTER TWO-TRAFFIC STREAM CHARACTERISTICS.....</b>	<b>2</b>
2.1 Background .....	2
2.2 Traffic Stream Parameters .....	3
2.2.1 Volume and Rate of Flow.....	3
2.2.2 Speed and Travel Time.....	4
2.2.3 Density and Occupancy .....	5
<b>CHAPTER THREE-LITERATURE REVIEW .....</b>	<b>7</b>
3.1 Traffic Flow Modeling .....	8
3.2 State Space Models and Filtering .....	11
3.2.1 Kalman Filter .....	12
3.2.2 Extended Kalman Filter .....	13
3.2.3 Unscented Kalman Filter .....	13
3.2.4 Particle Filter .....	14
3.3 Cell Transmission Model .....	16
3.4 Switching-Mode Model.....	19
<b>CHAPTER FOUR-PROPOSED TRAFFIC DENSITY ESTIMATION METHODS AND SIMULATION RESULTS.....</b>	<b>22</b>

4.1 Algorithms 1 and 2 Based on the First Method.....	26
4.1.1 Binary Estimation Method .....	29
4.1.1.1 Estimation for Single Road .....	29
4.1.1.2 Estimation for Adjacent Roads.....	30
4.1.2 Ternary Estimation Method.....	31
4.1.2.1 Estimation for Single Road .....	31
4.1.2.2 Estimation for Adjacent Roads.....	33
4.2 Algorithms 3 and 4 Based on Second Method .....	33
4.2.1 Binary Estimation Method .....	41
4.2.1.1 Estimation for Single Road .....	41
4.2.1.2 Estimation for Adjacent Roads.....	42
4.2.2 Ternary Estimation Method.....	42
4.2.2.1 Estimation for Single Road .....	43
4.2.2.2 Estimation for Adjacent Roads.....	43
4.3 Evaluation of Results.....	44
<b>CHAPTER FIVE-CONCLUSION.....</b>	<b>50</b>
<b>REFERENCES .....</b>	<b>53</b>



## LIST OF FIGURES

	<b>Page</b>
Figure 3.1 The freeway model of discrete section .....	9
Figure 3.2 Examples of density-speed fundamental diagrams.....	10
Figure 3.3 Flow parameter as a function of density.....	18
Figure 3.4 A segment of I-210W highway divided into cells .....	20
Figure 4.1 Illustration of binary prediction .....	24
Figure 4.2 Schema of algorithm 1 .....	27
Figure 4.3 Schema of algorithm 2.....	28
Figure 4.4 A two-state Markov Chain .....	35
Figure 4.5 Schema of algorithm 3.....	38
Figure 4.6 Schema of algorithm 4.....	40

## LIST OF TABLES

	<b>Page</b>
Table 4.1 Binary estimation results of algorithm 1 for single road .....	29
Table 4.2 Binary estimation results of algorithms 1 and 2 for adjacent roads.....	31
Table 4.3 Ternary estimation results of algorithms 1 and 2 for single road .....	32
Table 4.4 Ternary estimation results of algorithms 1 and 2 for adjacent roads .....	33
Table 4.5 Binary estimation results of algorithms 3 and 4 for single road .....	41
Table 4.6 Binary estimation results of algorithms 3 and 4 for adjacent roads.....	42
Table 4.7 Ternary estimation results of algorithms 3 and 4 for single road .....	43
Table 4.8 Ternary estimation results of algorithms 3 and 4 for adjacent roads .....	44
Table 4.9 Binary estimation results of the best algorithms for road 529 .....	46
Table 4.10 Confusion matrix of binary estimation for road 529 of algorithm 1.....	46
Table 4.11 Confusion matrix of binary estimation for road 529 of algorithm 4.....	46
Table 4.12 Binary estimation results of the best algorithms for adjacent roads .....	46
Table 4.13 Confusion matrix of binary estimation for adjacent roads of algorithm 2 .....	46
Table 4.14 Confusion matrix of binary estimation for adjacent roads of algorithm 3 .....	46
Table 4.15 Comparison of the best binary algorithms .....	47
Table 4.16 Ternary estimation results of the best algorithms for road 529 .....	47
Table 4.17 Confusion matrix of ternary estimation for road 529 of algorithm 2.....	47
Table 4.18 Confusion matrix of ternary estimation for road 529 of algorithm 4.....	47
Table 4.19 Ternary estimation results of the best algorithms for adjacent roads .....	47
Table 4.20 Confusion matrix of ternary estimation for adjacent roads of algorithm 2 .....	48
Table 4.21 Confusion matrix of ternary estimation for adjacent roads of algorithm 3 .....	48
Table 4.22 Comparison of the best ternary algorithms .....	48
Table 4.23 Comparison of the algorithm 1 and other prediction methods.....	49

## **CHAPTER ONE**

### **INTRODUCTION**

Today, one of the biggest problems of people living in the city is definitely the increasing vehicular traffic. With the increase of job opportunities and the ease of getting goods, thousands of vehicles are entering the traffic of big cities each day. By the impact of rush hours, or environmental factors such as rain and snow or traffic accidents, the problem of traffic density becomes even worse.

For finding solution to this problem, traffic control centers were established which use evolving technology such as loop detectors, GPS-enabled wireless devices, cameras, and various software and hardware devices. Traffic control centers aim to manage the traffic density and speed of the traffic flow and inform drivers with different applications such as density estimation map and traffic guidance by evaluating traffic data collected through these devices.

Here in this study we will concentrate on one of these applications which is traffic density estimation. First, in the second chapter, we will introduce the primary traffic parameters including density parameter which helps us to understand the traffic flow better. In the third chapter, we will briefly explain the density estimation methods widely used in many application areas in the literature. In the fourth chapter, we will introduce the proposed methods for density estimation based on algorithms frequently used in cognitive radio applications. At the end, we will discuss the performance of the proposed algorithms by using several performance evaluation criteria and also we will make suggestions for future studies.

## **CHAPTER TWO**

### **TRAFFIC STREAM CHARACTERISTICS**

#### **2.1 Background**

Traffic streams occur as a result of mutual effects of drivers and vehicles and their interaction with the physical elements of the roadway and its environment. Because driver behaviours and vehicle characteristics are different, manners of individual vehicles within the traffic stream are not exactly the same. In addition to these factors, there are also randomly occurring events such as accidents or changing weather conditions like rain, snow, icing on the road etc. Therefore, traffic involves an element of variability.

A water flow through channels and pipes of determined characteristics will behave in a completely predictable mode, in harmony with the laws of hydraulics and fluid flow. On the other hand a given traffic flow through streets and highways of specific characteristics will change with both time and location. Therefore, the critical problem of traffic engineering is to plan and design for a medium that is not presumable in exact terms-one that includes both physical limitations and the complex behavioral characteristics of human beings. Luckily, while exact characteristics change, there is a quite stable range of driver and, therefore, traffic stream behavior.

In explaining traffic streams in quantitative terms, the aim is to both understand the natural variability in their characteristics and to determine normal ranges of behavior. By doing so, key parameters must be determined and measured. Traffic engineers will examine, evaluate, and finally design improvements in traffic facilities depended on such parameters and their knowledge of normal ranges of behavior. In fact, these parameters are the traffic engineer's measurement of reality, and they compose a language with which traffic streams are understood and explained (Roess, Prassas & McShane, 2004). The following sections will summarize these parameters.

## **2.2 Traffic Stream Parameters**

Traffic stream parameters are divided into two wide categories. Macroscopic parameters explain the traffic stream completely; microscopic parameters explain the behavior of single vehicle or pairs of vehicles within the traffic streams.

The three principal macroscopic parameters that explain a traffic stream are (1) volume and rate of flow, (2) speed, and (3) density. Microscopic parameters contain (1) the speed of single vehicles, (2) headway, and (3) spacing. In this study, we only deal with macroscopic parameters.

### ***2.2.1 Volume and Rate of Flow***

Traffic volume is described as the number of vehicles passing a point on a highway, or on a given lane or direction of a highway, during a given time interval. The unit of measurement for volume is only “vehicles,” though it is often stated as “vehicles per unit time.” Units of time used frequently are “per day” or “per hour.”

Daily volumes are used to determine trends over time, and for general planning aims. Detailed plan or control decisions need information of hourly volumes for the peak hour(s) of the day.

Rates of flow are usually expressed in units of “vehicles per hour”, but indicate flows available for periods of time less than one hour. For example, a volume of 200 vehicles observed over a 15 minute period may be stated as a rate of  $200 \times 4 = 800$  vehicles/hour, even though 800 vehicles would not be observed in the full hour. The 800 vehicles/hour becomes a rate of flow available for a 15 minute interval (Roess et al., 2004).

### 2.2.2 Speed and Travel Time

Speed is the other macroscopic parameter explaining the state of a traffic stream. Speed is described as a rate of motions in distance per unit time. Travel time is the elapsed time in which a vehicle traverse a defined section of a roadway. Speed and travel time are inversely proportional:

$$S = d/t \quad (2.1)$$

where S is called speed, mi/h or ft/s

d is called distance traversed, in mile (mi) or feet (ft)

t is called time to traverse distance d, in hour (h) or second (s)

It is accepted that each vehicle travels at a different speed in a moving traffic stream. Therefore, the traffic stream does not have an individual characteristic value, but rather a distribution of individual speeds. The traffic stream, taken completely, can be described using an average or typical speed.

For a traffic stream, there are two ways in which an average speed can be calculated:

- Time mean speed (TMS): The average speed of all vehicles which pass a point on a highway or lane over some given time period.
- Space mean speed (SMS): The average speed of all vehicles which occupy a given section of highway or lane over some given time period.

In brief, TMS is a point measurement, while SMS indicates a length of highway or lane.

For measuring TMS, an observer standing by the side of the road would record the speed of each vehicle as it passes (Roess et al., 2004). For measuring SMS, an observer would require an elevated location from which the full area of the section

may be viewed. The SMS attaches importance to slower vehicles more heavily, depending on the amount of time they occupy a highway section. Therefore, the SMS is generally lower than the corresponding TMS, in which each vehicle is weighted equally. The two speed measures may reasonably be equal if all vehicles in the section are travelling at just the same speed.

TMS is calculated by finding each single vehicle speed and taking a simple average of the results. On the other hand, SMS is calculated by finding the average travel time for a vehicle to pass the section and using the average travel time to calculate a speed.

### ***2.2.3 Density and Occupancy***

Density, the last primary measurement of traffic stream characteristics, is described as the number of vehicles occupying a given length of highway or lane, generally stated as vehicles per mile or vehicles per mile per lane.

Density is difficult to measure directly, as an observer requires an elevated vantage point from highway section. It is often calculated from speed and flow rate measurements.

Density, however, is may be the most important of the primary stream parameters, since it is the measurement most directly related to traffic demand. Demand does not appear as a rate of flow, even though traffic engineers use density as the principal measurement of demand. Traffic is produced from various land uses, inserting a number of vehicles into a confined roadway space. This process composes a density of vehicles. Drivers choose speeds that are convenient with how close they are to other vehicles. The speed and density join to give the observed rate of flow (Roess et al., 2004).

Density is also an important measurement of quality of traffic flow, as it is a factor which affects freedom to maneuver and the psychological comfort of drivers.

While density is difficult to be measured, modern detectors can measure occupancy, which is closely related with density. Occupancy is defined as the proportion of time that a detector is “occupied”, or covered, by a vehicle in a given time period.

Occupancy is measured for a specific detector in a particular lane. Therefore, the density estimated from occupancy is in units of vehicles per mile per lane. If there are neighboring detectors in extra lanes, the density in each lane may be added to provide a density in veh/mi for a given direction of flow over several lanes (Roess et al., 2004).



## **CHAPTER THREE**

### **LITERATURE REVIEW**

As mentioned in the previous sections, density is the most important primary traffic parameter since it provides the maximum information about the traffic situation. Therefore, traffic control centers, which aim to monitor the traffic of the city, collect the necessary traffic information and usually report this information to drivers as the density parameter. Traffic control centers using parameters such as speed, flow rate, the number of vehicles in one lane, past density information etc. from provided data, try to estimate the density by different methods. In this section we will examine the most commonly used methods for density estimation.

Alvarez-Icaza et al. have made density estimation by using traffic flow model derived from the studies of (Lighthill & Whitham, 1955) and (Richards, 1956). This model is named LWR which is the base of many traffic engineering studies. A proposed traffic density design is used for real time on-ramp metering control for freeways. The design can be used in two situations: a) when there are no traffic flow sensors properly located, and b) when available sensors have several errors. These two problems require to arrange traffic estimation design to recover the missing information. In (Alvarez-Icaza, Munoz, Sun & Horowitz, 2004) an estimation design for vehicle density in the middle section of a stretch of freeway is presented. It is assumed that traffic flow at the entry and exit of that section is known. The design is based on a conservancy of vehicles model and a speed-density relationship given by “fundamental diagrams.” A nonlinear observer is arranged that uses the model structure to set a matrix of observer gains. Together with the design of the observer, it is suitable to estimate some traffic mixing factors that appear during the spatial discretization of the conservation of vehicles model and whose value indicates the traffic state: free or congested (Alvarez-Icaza et al., 2004).

### 3.1 Traffic Flow Modeling

Traffic flow modeling depends on a conservation of vehicles principle that can be expressed as

$$\frac{\partial N(x,t)}{\partial t} = - \frac{\partial}{\partial x} \{V(x,t)N(x,t)\} \quad (3.1)$$

where  $x$  is called the longitudinal position along the freeway,  $t$  is the time,  $N(x, t)$  is the vehicle density at position  $x$  and time  $t$  and  $V(x, t)$  is the longitudinal speed. Both quantities  $N(x, t)$  and  $V(x, t)$  are collected for all the freeway lanes.

The model in Equation (3.1) can be discretized in a set of finite length sections, if the equation is integrated with respect to  $x$  in both sides. For this integration, upstream or downstream boundary conditions should be taken into account, based on the traffic state being free or congested. Figure 3.1 indicates a schematic diagram of a four section freeway where the integration has been made using upstream boundary conditions (Alvarez-Icaza et al., 2004). The suitable model has the form

$$\dot{n}_1 = \frac{1}{L_1} (q_{in} - q_1) \quad (3.2)$$

$$\dot{n}_2 = \frac{1}{L_2} (q_1 - q_2) \quad (3.3)$$

$$\dot{n}_3 = \frac{1}{L_3} (q_2 - q_3) \quad (3.4)$$

$$\dot{n}_4 = \frac{1}{L_4} (q_3 - q_4) \quad (3.5)$$

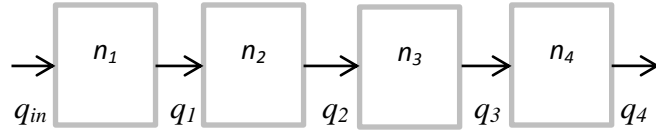


Figure 3.1 The freeway model of discrete section

where  $n_i$  is called the average vehicle density in section  $i$ ,  $L_i$  is the length of section  $i$ ,  $q_i$  is the flow between sections  $i$  and  $i + 1$ , and  $q_{in}$  is the inflow to the first section. Succession of models as the one in Equations (3.2)-(3.5) makes it possible to plan more complex freeway networks. The flow  $q_i$  in the model of Equations (3.2)-(3.5) can be stated as

$$q_i = n_{qi} v_{qi} \quad (3.6)$$

where  $n_{qi}$  and  $v_{qi}$  are the density and speed in the point where sections  $i$  and  $i + 1$  adjoin. While for a general case of a hydrodynamic system, speed and density are independent variables, for transportation systems there is plentiful literature about the situation in that drivers adjust their speed depending on the density they perceive locally. This speed-density relationship is expressed through what is known as “fundamental diagrams.” Figure 3.2 indicates two curves that match to two different fundamental diagrams. Two parts can be separated in the curves. In the first part, that matches to low densities, speed is constant and characterizes free flow state where drivers travel at the maximum permissible speed. The second part of the curve, for higher densities, indicates a decreasing value of speed with the increase of density when the traffic is congested. In the first example shown in Figure 3.2, speed decreases linearly with density, when this goes beyond a critical value, until getting to the point of traffic jam, where speed is zero. In the second example, a driver decreases its speed as a function of the square of the distance between him/her and the driver in front. The distance is inversely proportional to density: more density means less distance between vehicles and therefore smaller speeds (Alvarez-Icaza et al., 2004).

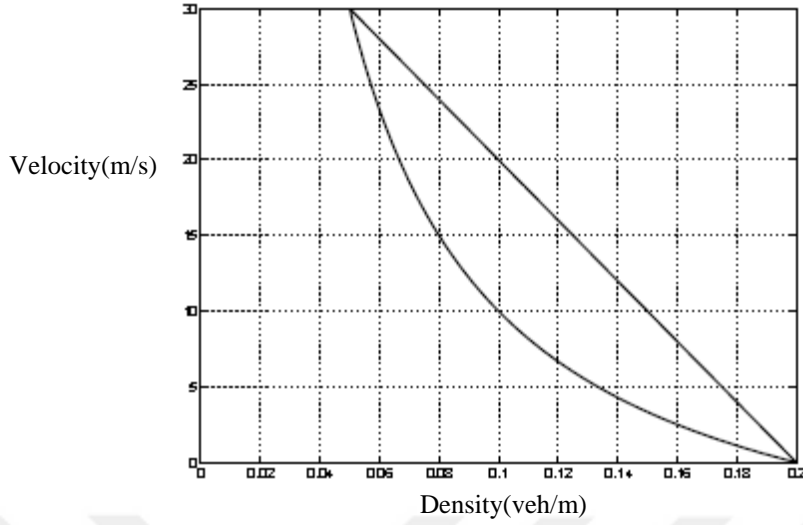


Figure 3.2 Examples of density-speed fundamental diagrams (Alvarez-Icaza et al., 2004)

$n_i$  is used to model the average density in section  $i$  in Equations (3.2)-(3.5), when density  $n_{qi}$  in the point adjoining section  $i$  and  $i+1$ , was used in Equation (3.7)-(3.10). Therefore it is essential to express  $n_{qi}$  as a function of  $n_i$ , and to this end it is proposed to model flow  $q_i$  according to

$$q_1 = (\alpha_1 n_1 + (1 - \alpha_1) n_2) v_{q1} \quad (3.7)$$

$$q_2 = (\alpha_2 n_2 + (1 - \alpha_2) n_3) v_{q2} \quad (3.8)$$

$$q_3 = (\alpha_3 n_3 + (1 - \alpha_3) n_4) v_{q3} \quad (3.9)$$

$$q_4 = n_4 v_{q4} \quad (3.10)$$

where  $\alpha_i \in [0, 1]$  are mixing factors with regard to the length of sections  $i$  and  $i + 1$  and the traffic state: free or congested. In (Alvarez-Icaza et al., 2004) these factors are considered unknown and constant for each traffic state. The terms in parantheses in the right side of Equations (3.7)-(3.10) mean that density  $n_{qi}$  is a convex mixing of the average densities  $n_i$  in the adjacent sections. Speed  $v_{qi}$  is either known or can be computed from a fundamental diagram based on the values of  $n_i$  and  $\alpha_i$ .

If Equations (3.2)-(3.5) and (3.7)-(3.10) are designed in matrix form, they become

$$\dot{N} = L_{in}V_qA_\alpha N + Bq_{in} \quad (3.11)$$

A proposed algorithm by (Alvarez-Icaza et al., 2004) is used to estimate vehicle density in conditions where the sensor is not in the location along the freeway or is faulty. The design was depended on a conservation of vehicles model and considered the existence of a fundamental diagram describing the speed-density relationship. From this, an adaptive observer is proposed whose stable behavior is based on the choice of a gain matrix in accordance with traffic state: free or congested. The design was demonstrated with simulations that confirm analytical findings. The design can be applied to more complex scenarios and combined with on-ramp metering control algorithms (Alvarez-Icaza et al., 2004).

Kalman filter is undoubtedly one of the most widely used methods to estimate not only density but also speed and travel time parameters (Ye, 2007; Qiu, 2007; Chu, 2005; Yang, 2012).

Yang pays attention to develop a traffic state estimation algorithm for the specific stochastic traffic flow model. He shows that the discretized version of the stochastic traffic flow model can be rearranged as a state space model and nonlinear Kalman filter algorithms can be implemented. After then, by comparing the estimation accuracy of the traffic flow model with and without the on-line algorithm, he shows that on-line algorithm is able to improve the estimation performance of the future traffic state.

### **3.2 State Space Models and Filtering**

A state space model is given by Equations (3.12) and (3.13). Equation (3.12) is the state transition equation of the state space model.  $x_k$  is the state variable of the system at time  $k$  and  $w_k$  is the transition disturbance. We can obviously see from the

state transition equation that the state variable in the current period is dependent on the previous state and the disturbance. Equation (3.13) is the observation equation, where  $z_k$  is observation variable and  $\epsilon_k$  is the measurement noise. In state estimation, the transition and observation equations are both given. The observation variable  $z_k$  is measured at all time periods. The aim of these equations is to make the best estimation of  $x_k$  which is based on historical observations of  $z_k$ .

$$x_k = f_k(x_{k-1}, w_k) \quad (3.12)$$

$$z_k = h_k(x_k, \epsilon_k) \quad (3.13)$$

### 3.2.1 Kalman Filter

When  $F_k$  and  $H_k$  are both linear functions as shown in Equation (3.14) and (3.15), and  $w_k, \epsilon_k$  are distributed independently with normal distribution:  $w_k \sim N(0, Q_k)$  and  $\epsilon_k \sim N(0, R_k)$ , then the state space model is linear and it is known that Kalman filter (Kalman, 1960) will make the best estimation of  $x_k$  under this situation.

$$x_k = F_k x_{k-1} + w_k \quad (3.14)$$

$$z_k = H_k x_k + \epsilon_k \quad (3.15)$$

Let  $\hat{x}_{k/k}$  show a posterior estimation of state  $x_k$  at  $k^{th}$  time instant given observations up to and including at time  $k$ , and  $P_{k/k}$  show a posterior error covariance matrix of the state estimation at  $k^{th}$  time instant (Yang, 2012). Let  $\hat{x}_{k/k-1}$  show a priori estimation of state  $x_k$  at  $k-1^{th}$  time instant given observations up to and including at time  $k-1$ , and  $P_{k/k-1}$  show a priori error covariance matrix of the state estimation at  $k-1^{th}$  time instant.

Kalman filter rearranges the posterior distribution of the state after taking the observation information according to Equations (3.16)-(3.20)

$$y_k = z_k - H_k \hat{x}_{k/k-1} \quad (3.16)$$

$$S_k = H_k P_{k/k-1} H_k^T + R_k \quad (3.17)$$

$$K_k = P_{k/k-1} H_k^T S_k^{-1} \quad (3.18)$$

$$\hat{x}_{k/k} = \hat{x}_{k/k-1} + K_k y_k \quad (3.19)$$

$$P_{k/k} = (I - K_k H_k) P_{k/k-1} \quad (3.20)$$

Kalman filter gives the best estimation for linear state space model. However for the stochastic traffic flow model, because of the complexity of the model, both  $F_k$  and  $H_k$  are nonlinear. Kalman filter is not good at stochastic traffic flow model therefore nonlinear Kalman filter has to be applied.

### ***3.2.2 Extended Kalman Filter***

Extended Kalman filter (EKF) is a commonly used nonlinear filtering algorithm for models like in Equations (3.12) and (3.13) where both  $F_k$  and  $H_k$  are nonlinear functions. It has been frequently used in practice because of its simplicity. The main idea of EKF is linearization of the transition equation and measurement equation around the current estimated state. Then Kalman filter can be applied to make an estimation of the approximated linear model. When EKF is compared with the procedure of Kalman filter, it is very similar except some slight differences in the predict and update states (Yang, 2012).

### ***3.2.3 Unscented Kalman Filter***

Unscented Kalman filter (UKF) is a nonlinear Kalman filter which gives better estimation than EKF when the transition equation is highly nonlinear. In EKF, the priori distribution of the state variable is estimated by a Gaussian distribution. There is a poor approximation when the transition equation is highly nonlinear. Moreover

UKF does not calculate the derivative, because of this, it is more efficient than EKF in the case where the state variable is high dimensional. With those two advantages, UKF might be a better estimator for the on-line traffic state estimation.

The main idea of UKF is unscented transform. Unscented transform is a mathematical sampling method for estimating the mean and covariance matrix of the output variable from a non-linear transformation of the input variable, given the mean and covariance matrix of the input variable. UKF initially produces a set of sample points (called sigma points). Each sigma point is related with a corresponding weight, from the mean and covariance matrix of the input random variable by using unscented transform. Each sigma point is a performed input of the non-linear function. The set of sigma points is spreaded through the non-linear function to produce a set of sample outputs, thus the mean and covariance matrix of the output variable could be estimated from these sample outputs (Yang, 2012).

#### ***3.2.4 Particle Filter***

Particle filter (PF) is used as sequential Monte Carlo method for highly non-linear and complicated transition and measurement equations (Qiu, 2007). Like UKF, PF estimates the posterior probability distribution of the state variable by a set of particles (sample points): In the first step, a set of particles with equal weights are taken from the prior probability distribution of the state. Then the particles are modified by Monte Carlo simulation according to the transition equation. Each particle denotes one path of the state variable and the weight denotes the probability of the occurrence of this path. When new information is taken at each time step, PF updates the weights of all the particles. When the number of particles is large enough, the rearranged discrete distribution of the particles estimates the posterior probability distribution of the state. A resampling procedure is used at some points of time in order to keep variety among the particles.

The synthetic traffic flow data used in (Yang, 2012) are produced by simulation from noisy measurement data in a subset of the cells. The performances of UKF and



PF in terms of their abilities are evaluated by these data for estimating the true traffic state in all the cells over the highway. It is considered that the model parameters are known in this numerical experiment.

The estimation of the traffic density without any filtering is computed by dividing the measured volume by measured speed. Both PF and UKF estimate the true state very closely in all the cells. While the speed is low due to the high density in that location, the noise measured in the speed will have much higher effect to the estimated density than the condition when the speed is high. Also the measurement noise of speed will be increasing as the density increases because of the fact that the density is not a continuous variable. Hence, when traffic gets congested, the simple estimation will not work properly and filtering algorithms, such as UKF and PF, can maintain the estimation error (Yang, 2012).

The performance of the simple estimation is related with the traffic congestion level. As the traffic is extremely congested, the error of no filtering estimation is much larger than that of UKF and PF. As the traffic is under free flow condition, the error of no filtering estimation is similar to that of UKF and PF.

Finally, it can be said that if the model parameters are known, UKF and PF can improve the estimation accuracy of the traffic state especially in the congested traffic (Yang, 2012).

In (Munoz, Sun, Horowitz & Alvarez, 2003) a macroscopic traffic flow model, called the switching mode model (SMM), has been produced by the cell transmission model (CTM) and then implemented to the traffic density estimation at unmonitored locations along a highway. The SMM is a hybrid system that changes between different sets of linear difference equations, or modes, based on the mainline boundary data and the congestion status of the cells in a highway section (Munoz et al., 2003).

### 3.3 Cell Transmission Model

The Lighthill-Whitham-Richards model (Lighthill & Whitham, 1955; Richards, 1956), often referred to as LWR model, contains a vehicle conservation equation

$$\frac{\partial \rho(x,t)}{\partial t} + \frac{\partial q(x,t)}{\partial x} = 0 \quad (3.21)$$

and a static flow-density equation

$$q(x,t) = Q(\rho(x,t)) \quad (3.22)$$

which is frequently called the basic diagram in traffic engineering. Because of different presumptions about traffic behaviors and better fit for the measured data, researchers have suggested many basic diagrams of different shapes (Sun, 2005). But they all use the following characteristics:

1.  $Q(0) = Q(\rho_J) = 0$ , where  $\rho_J$  is the jam density.
2.  $Q(\rho)$  is a concave function which is given in Figure 3.3.
3.  $Q(\rho)$  reaches its maximum  $Q_M$ , which is the capacity, at  $\rho_c$ , the critical density.

The cell transmission model (CTM) improved by Daganzo, is a finite difference approach to the LWR model, which makes it a first-order discrete model (Daganzo, 1995a; 1995b).

The CTM uses the LWR model in time by selecting a time step  $\Delta t$  and in space by separating a road segment into small sections, or cells, of uniform lengths  $l$ . The CTM was expanded in (Daganzo, 1995a) to contain a more general road topology that includes merging and diverging flows. It was further concerted in (Daganzo, 1995a) to accommodate nonuniform cell lengths. In spite of the relative simplicity and approach of the CTM, it still captures the shock behavior estimated by the LWR model and derives important traffic phenomena, such as backward propagation of congestion waves.

The cell transmission model, a macroscopic traffic model, was chosen for (Munoz et al., 2003) because of its analytical simplicity and capability of reproducing congestion wave propagation dynamics. The modified CTM, from which the SMM is reproduced, (1) uses cell densities as state variables instead of cell occupancies, (2) approves nonuniform cell lengths, and (3) approves congested conditions to be preserved at the downstream boundary of a modeled freeway section.

Using cell densities instead of cell occupancies allows the CTM to contain uneven cell lengths, which guides to greater flexibility in partitioning the highway. Lengths of nonuniform cells also allow us to use a smaller number of cells to describe a given highway segment, thus decreasing the size of the state vector  $[\rho_1, \dots, \rho_N]^T$ , where  $\rho_i$  is the density of the  $i$ th cell. When it is expected that separating a segment into a large number of cells can make better numerical accuracy, our attention here is testing our methods by using a smaller state vector and simplifying the design of estimators and controllers. Permitting congested flow rates at downstream boundaries is essential to enable the model to work with real highway data.

A highway is divided into a series of cells in the modified CTM. The density of cell  $i$  is modified with conservation of vehicles. If there are no on- or off-ramps in linear highway segment, vehicle conservation can be written as

$$\rho_i(k+1) = \rho_i(k) + \frac{T_s}{l_i}(q_i(k) - q_{i+1}(k)) \quad (3.23)$$

$k$  is called the time index,  $T_s$  is called the discrete time interval,  $l_i$  is the length of cell  $i$ , and  $q_i(k)$  is defined as the flow rate, in vehicles per unit time, into cell  $i$  during the interval  $[k, k+1)$ .  $q_i(k)$  is defined by taking the minimum of two quantities:

$$q_i(k) = \min(S_{i-1}(k), R_i(k)) \quad (3.24)$$

where  $S_{i-1}(k) = \min(v\rho_{i-1}(k), Q_{M,i-1})$  is the maximum flow which can be received by cell  $i-1$  under freeflow conditions, over the interval  $[k, k+1)$ , and  $R_i(k) = \min(Q_{M,i}$

$w(\rho_J - \rho_i(k))$ , is the maximum flow that can be supplied by cell  $i$  under congested conditions, over the same time interval. Equations (3.23) and (3.24) are the density-based equivalents. The modified CTM also uses density-based versions of the merge and diverge laws to combine on-ramp and off-ramp traffic (Munoz et al., 2003).

The CTM parameters are described in the basic diagram of Figure 3.3. They can be acceptable for all cells or permitted to vary for each cell. The free-flow speed  $v$  is the average speed at which vehicles move on the highway under uncongested (low density) state.  $w$  is the average speed at which congestion waves spread upstream through the highway under fully congested state.

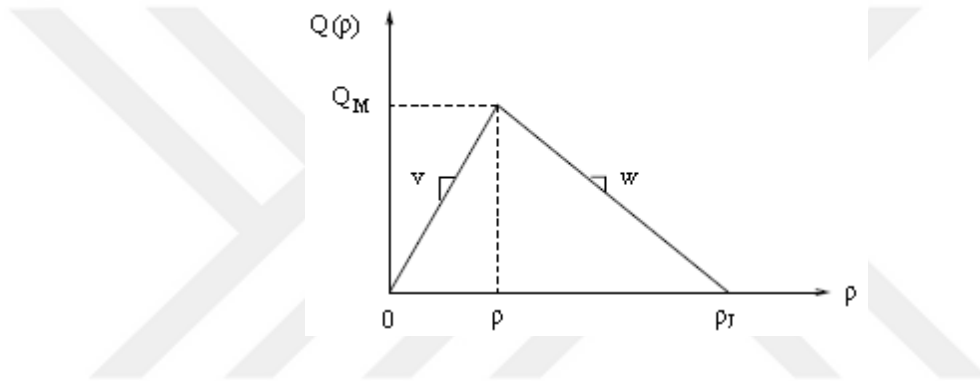


Figure 3.3 Flow parameter as a function of density (Munoz et al., 2003)

The congestion status of cell  $i$  is defined by comparing the cell density with the critical density: if  $\rho_i < \rho_{c,i}$  the cell has free-flow state, otherwise  $\rho_i \geq \rho_{c,i}$  and the cell has congested state. The SMM changes between each other several sets of linear difference equations based on the values of the mainline boundary inputs and on the congestion state of the cells in a section. Each set of linear equations belongs to a mode of the SMM. The SMM predicts the movement of congestion wave fronts through a highway section. A wave front is defined as a status transition, upstream of which nearby cells have one state (e.g. free-flow), and downstream of which nearby cells have the opposite state.

### 3.4 Switching-Mode Model

In the SMM, the cell transmission model is described as a hybrid system that switches between 5 sets of linear difference equations, based on the congestion state of the cells and the values of the mainline boundary data. Considering our state variable is the cell densities,  $\rho = [\rho_1, \dots, \rho_N]^T$ , the main difference between the CTM and the SMM is that, with respect to density, the former is nonlinear, whereas each mode of the latter is linear. The SMM can be derived from the modified CTM by writing each inter-cellular flow,  $q_i$ , as either an apparent function of cell density,  $v_{\rho_{i-1}}(k)$  or  $w(\rho_j - \rho_i(k))$ , or as a constant,  $Q_M$ . This apparent density dependence is achieved by supplying a set of logical rules that define the congestion state of each cell, at every time step, depending on measurements at the segment boundaries (Munoz et al., 2003).

For simplicity, the following presumptions are made:

1. The densities and flows at the upstream and downstream segment boundaries, including flows on all the on-ramps and off-ramps, are measured.
2. There is at most one state transition (or wave front) in the highway section. If both the upstream and downstream mainline boundaries are at the same state, i.e., both free-flow or both congested, it is considered that all the mainline cells, 1 through N, have the same state. If the two boundaries are at different states, there exists a single wave front in the segment, upstream of which all the cells have congested (free-flow) state, and downstream of which all the cells have free-flow (congested) state.

Since an SMM-modeled section includes at most one congestion wave front, the modes of the SMM can be discriminated by the congestion state of the cells upstream and downstream of the wave front. If there is no wave front in the section, doubled label can be used, e.g. “Free-flow– Free-flow” to show the absence of any status transition. The five modes are indicated: (1) “Free-flow–Free-flow” (FF), (2) “Congestion–Congestion” (CC), (3) “Congestion– Free-flow” (CF), (4) “Free-flow–

Congestion 1” (FC1), and (5) “Free-flow–Congestion 2” (FC2). The first state of “Free-flow–Congestion” is defined as the magnitude of the supplied flow of the last uncongested cell upstream of the wave front. The second state is defined as the magnitude of the receiving flow of the first congested cell downstream of the wave front. If the first one is larger, the SMM is in FC1; and if the second one is larger, it is in FC2. Respectively, these two cases are discriminated by whether the congestion wave is going backward or forward within the segment. The highway segment is shown in Figure 3.4, which is separated into 8 cells (Munoz et al., 2003).

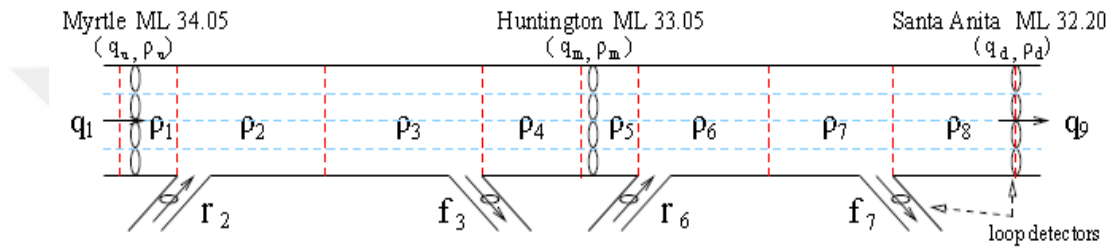


Figure 3.4 A segment of I-210W highway divided into cells (Munoz et al., 2003)

The measured total flows and densities at the upstream and downstream mainline detectors are indicated by  $q_u, \rho_u$ , and  $q_d, \rho_d$ . All five modes of the SMM can be shown as follows:

$$\rho(k+1) = A_s \rho(k) + B_s u(k) + B_{J,s} B_{Q,s} \rho_J + B_{Q,s} Q_m \quad (3.25)$$

where  $s = 1, 2, 3, 4, 5$  denotes the mode (1: FF, 2: CC, 3: CF, 4: FC1, 5: FC2),  $\rho = [\rho_1 \dots \rho_4]^T$  is the status, and  $u = [q_u \ r_2 \ f_3 \ \rho_d]^T$  are the flow and density inputs; specifically,  $r_2$  and  $f_3$  are the measured on-ramp and off-ramp flows entering and leaving the section, as written according to their cell of entry or exit.  $\rho_J = [\rho_{J1} \ \rho_{J2} \ \rho_{J3} \ \rho_{J4} \ \rho_{J5}]^T$  is the jam densities vector, and  $q_m = [Q_{M1} \ Q_{M2} \ Q_{M3} \ Q_{M4}]^T$  is the maximum flow rates vector.

At each time step, the SMM defines its mode depending on the measured mainline boundary data and the congestion state of the cells in the section. If both  $\rho_u$  and  $\rho_d$

have free-flow status, the FF mode is chosen, and if both of these densities are congested, the CC mode is chosen. If  $\rho_u$  and  $\rho_d$  are of opposite state, then the SMM makes a search over the  $\rho_i$  to define whether there is a state transition inside the section. This wave front search looks for the first status transition between adjacent cells (Munoz et al., 2003).

We make several presumptions in order to contact the measured quantities ( $q_u, \rho_u, q_m, \rho_m, q_d, \rho_d$ , and flows measured at each on- and off-ramp) to flows and densities used by the model: (1)  $\rho_u$  is a density measurement in the first cell, i.e.  $\rho_u = \rho_1$ ; (2) similarly,  $\rho_d = \rho_8$ ; (3) A measurement of  $\rho_5$  is the middle density  $\rho_m$ , since the middle mainline station (Huntington) is placed within cell 5; (4)  $r_i$  (or  $f_j$ ) is equal to the measurement of on-ramp (or off-ramp) flow at the corresponding on-ramp (or off-ramp) station.

Both the SMM and modified CTM were simulated for the section in Figure 3.4 using data obtained from I-210 West for several weekdays, over the interval 5AM-12PM, during the morning rush-hour congestion state. It was considered that the upstream and downstream mainline data ( $q_u, \rho_u, q_d, \rho_d$ ), including the ramp flow data, were known. On the other hand, the middle density,  $\rho_m$ , was an estimated parameter. The purpose of the simulation was to determine whether the models could accurately estimate  $\rho_m$ .

The mean percentage error is defined as;

$$E_{MPE} = \frac{1}{M} \sum_{k=1}^M \left| \frac{\rho_m(k) - \hat{\rho}_m(k)}{\rho_m(k)} \right| \quad (3.26)$$

The mean percentage error over five different days in 2001 is nearly 13%. The results show that both the SMM and modified CTM have a good estimate of  $\rho_m$ . The accuracy of the two models is quite similar (Munoz et al., 2003).

## CHAPTER FOUR

### PROPOSED TRAFFIC DENSITY ESTIMATION METHODS AND SIMULATION RESULTS

We examined the most frequently used density estimation methods in the previous chapter. While these methods use traffic parameters such as flow speed, previous density, speed, lane number in estimation, the proposed density estimation methods in this study use only the past density information. Proposed methods are inspired by a similar problem in cognitive radio (CR) applications namely estimation of the status of a slot as busy or available to prevent the simultaneous usage of primary user and secondary user.

In the following subsections we will briefly explain the working principles of related studies for cognitive radio applications. Then, we will explain our proposed methods inspired by these studies for traffic density estimation.

In cognitive radio studies there are three types of prediction problem in the literature:

**Spectrum Prediction:** In this prediction problem, the status of the allocated spectrum and location of spectral holes for future periods are estimated by interpreting the past decisions or information (Black, Kerans & Kerans, 2012).

**Primary User (PU) Traffic Pattern Prediction:** For this problem, channel traffic parameters (state transition probability, arrival rate, etc.) are estimated first. Then, a decision is made by using these estimated parameters about whether the primary user (PU) will be in the channel or not for the next sensing period. (Chun-Hao, Gabran & Cabric, 2012)

Chun-Hao et al. (2012) explains the methods used for traffic estimation and prediction. A single channel randomly accessed by a single PU is considered, where the traffic of the PU is considered to be stationary. Furthermore, the PU ON/OFF



intervals are considered to be exponentially distributed (Wilkomm, Machiraju, Bolot & Wolisz, 2008; Lopez-Benitez & Casadevall, 2011; Kim & Shin, 2008), where the probability density function of the interval,  $t$ , is shown as

$$f_{\lambda}(t) = \begin{cases} \lambda e^{-\lambda t}, & \text{for } t \geq 0 \\ 0, & \text{otherwise} \end{cases} \quad (4.1)$$

with  $\lambda$  is  $\lambda_n$  and  $\lambda$  is  $\lambda_f$  for the ON and OFF periods, respectively. Because of a property of exponential distributions, the means of the ON and OFF intervals are equal to the reciprocals of  $\lambda_n$  and  $\lambda_f$ , respectively. The duty cycle  $u$  is described as  $u = \frac{\lambda_f}{\lambda_f + \lambda_n}$ , denoting the fraction of time with the existence of PU. Duty cycle also indicates the channel usage, which is the key parameter for traffic estimation.

The PU traffic usage is modeled as a semi-Markov process  $s_i$  (Kim & Shin, 2008), where  $s_i$  indicates the status of the PU as absent or present. The traffic is explained by a stationary distribution and the transition probabilities. The former represents the probabilities of the PU being absent and present at time  $T_i$ , with  $\Pr\{s_i = 0\} = P_0 = 1 - u$  and  $\Pr\{s_i = 1\} = P_1 = u$ . The later represents the probability of changing from state  $x$  to  $y$  during arbitrary time interval  $T_c$  (Chun-Hao et al., 2012). The probabilities of the four possible transitions are shown as

$$P_{00}(T_c) = 1 - u(1 - E) \quad (4.2)$$

$$P_{01}(T_c) = u(1 - E) \quad (4.3)$$

$$P_{10}(T_c) = (1 - u)(1 - E) \quad (4.4)$$

$$P_{11}(T_c) = u(1 - E) + E \quad (4.5)$$

where  $E = e^{-(\lambda_f + \lambda_n)T_c}$ .

The traffic parameters are predicted by using the results of spectrum sensing measured at time  $N$  in (Chun-Hao et al., 2012). Spectrum sensing is considered to be perfect. Then the proposed algorithm of (Chun-Hao et al., 2012) predicts the future PU state  $\hat{s}_{i+1}$  depending on the estimated parameters  $\{\hat{\lambda}_f, \hat{\lambda}_n, \hat{u}\}$  and the current PU state  $s_i$ . The effect of estimation errors on the prediction error rate is analyzed, and prediction regions which quantify the prediction confidence are defined.

**Binary Estimation:** In this method, past spectral decisions about channel states are the inputs of the prediction algorithm. This is also the main subject which will be discussed in this study. The purpose is to give a binary state to the PU for the next period using previously estimated binary states. An illustration for binary prediction is shown in Figure 4.1.

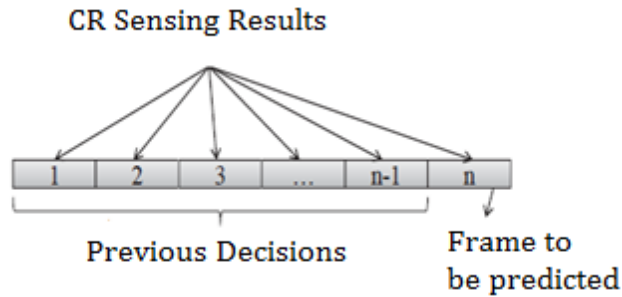


Figure 4.1 Illustration of binary prediction (Düzenli, 2015)

Two new parameters used in our algorithms are introduced below:

**History Window ( $W_H$ ):** History window includes the binary decisions (0 or 1) acquired in the previous sensing periods where 0 means channel is idle and 1 means channel is being used by the PU. The length of history window changes as 5, 10, 20, and 30 as stated in (Uyanık, Canberk & Oktuğ, 2012).

**Prediction Window ( $W_P$ ):** Prediction window indicates over how many time slots the prediction is carried out.

Considering these two parameters, the prediction methods used in (Uyanık et al., 2012) can be summarized as follows:

**Correlation-Based Prediction Method:** Pearson correlation coefficient is calculated using the past decisions given in history window as below (Canberk, Akyildiz & Oktug, 2011; Rodgers & Nicewander, 1988).

$$P(\underline{x}^{(n)}, \underline{r}^{(n)}) = \frac{1}{n-1} \sum_{i=1}^n \left[ \frac{x(i) - E[\underline{x}^{(n)}]}{\sigma_{\underline{x}^{(n)}}} \right] \times \left[ \frac{r(i) - E[\underline{r}^{(n)}]}{\sigma_{\underline{r}^{(n)}}} \right] \quad (4.6)$$

where  $\underline{x}^n$  indicates the sample index vector,  $\underline{r}^n$  shows the modeled PU activity sample vector,  $E[\cdot]$  is the mean, and  $\sigma$  is the standard deviation. If correlation coefficient is lower than the defined threshold, the majority value in history window is given as the future value, if correlation coefficient is higher, future value is the latest slot of history window.

**Correlation and Linear Regression based Prediction Method:** In this prediction design, Pearson correlation coefficient is acquired and compared with the defined threshold again. If it is greater than the threshold which refers to presence of a linear relation among the decisions in history window, then linear regression is performed to data in history window to estimate the state of the channel for the next period. The results of linear regression are converted into binary data comparing them with a threshold value of 0.5. If results are lower than 0.5, the future value is 0, if they are greater than 0.5, the future value is 1. If correlation coefficient is lower than the threshold, then the majority result is given as the next decision as in correlation based prediction design (Düzenli, 2015).

**Autocorrelation based Prediction Method:** According to this method, autocorrelation of the binary data in history window is calculated for different lags ( $l=1, 2, \dots, WH/2$ ). When lag is equal to 0, the autocorrelation coefficient will be equal to 1. In this method, the property of autocorrelation function given as the next maximum of auto-correlation coefficient's lag number denotes the periodicity. If a

repeating pattern exists in history window, then it is used for prediction of the next period.

#### 4.1 Algorithms 1 and 2 Based on the First Method

According to this method, the traffic parameters are acquired from the history window using the parameters defined below:

- **arrival\_rate:** Number of 0-1 transitions in the history window/History window length
- **departure\_rate:** Number of 1-0 transitions in the history window/History window length
- **last\_active\_slot:** Slot of the last sample of history window where the decision is 1
- **last\_idle\_slot:** Slot of the last sample of history window where the decision is 0

The reciprocal of the `arrival_rate` and `departure_rate` indicate the *mean busy* and *idle durations*, respectively (Kay, 2006). This method is summarized in **Algorithm 1** below.

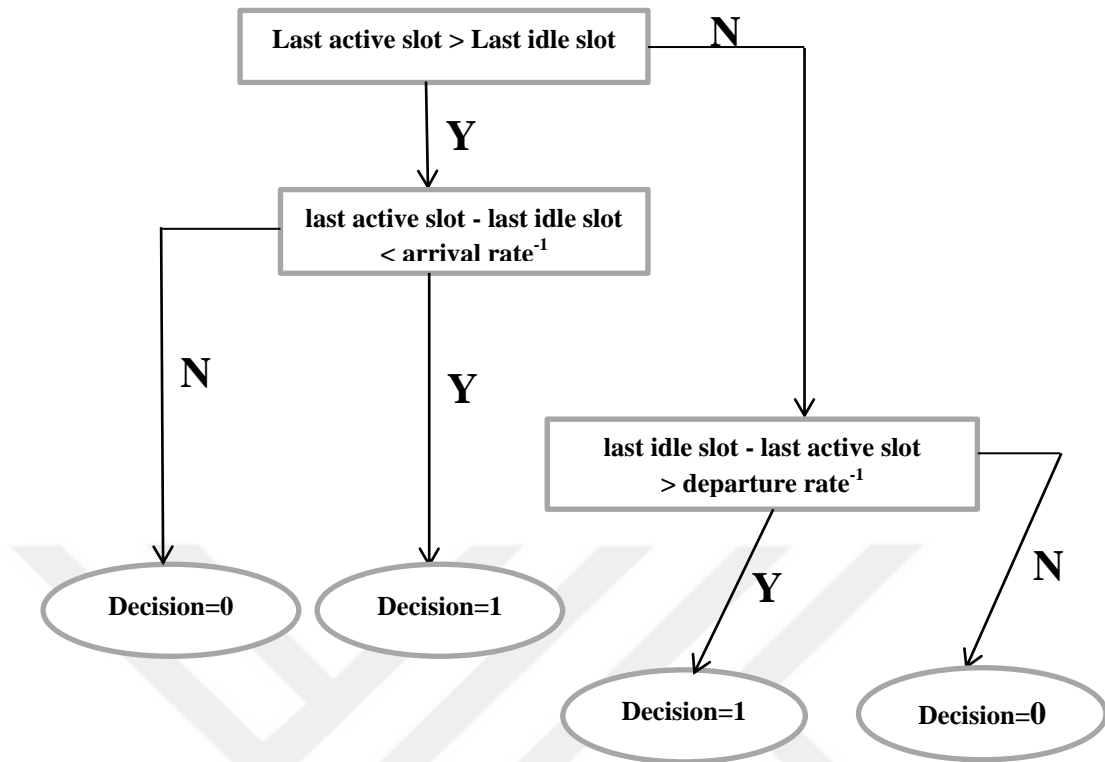


Figure 4.2 Schema of algorithm 1

First in Algorithm 1, we have defined vector cluster which is named temp and used for taking sample at history window length from data in the first section of the algorithm. Then we have found the place of the last 1 and 0 (last active slot and last idle slot) in temp window.

In the second section of the algorithm we have added one to arrival rate parameter if there is a transition from zero to one. Then, we have added one to departure rate parameter if there is a transition from one to zero. When total arrival rate and departure rate are counted, they are divided by the history window length Wh.

In the third section of the algorithm, it can be seen that the channel will incline to be busy if last\_active\_slot is greater than last\_idle\_slot and the length of the samples between last\_active\_slot and last\_idle\_slot is smaller than *mean busy duration* of the PU. On the other hand, if last\_idle\_slot is greater than last\_active\_slot and the length

of the samples between last\_idle\_slot and last\_active\_slot is smaller than *mean idle duration* of the PU, than the decision for the next period will incline to be idle again.

In the fourth section of algorithm, if binary data is 0 and decision slot is 0, we have added one to true positive parameter. Total true positive is the value which shows how much zero we have estimated truly. If binary data is 1 and decision slot is 1, we have added one to true negative parameter. When we have divided total true positive to total number of 0 and we have divided total true negative to total number of 1, we have found the values of true positive ratio and true negative ratio, respectively. Success parameter corresponds to addition of total true positive and total true negative. We have computed total accuracy with dividing success to total number of ones and zeros.

But when Algorithm 1 is used with converted ternary data, we observed that one and two positive ratio obviously are lower than zero positive ratio. So we have revised our algorithm as Algorithm 2. In Algorithm 2, if there are at least three consecutive identical data between last five data, our decision is that binary value. For example, if last five data is 0, 1, 2, 2, 2, our estimated data is 2. This method is summarized in **Algorithm 2** for binary estimation below.

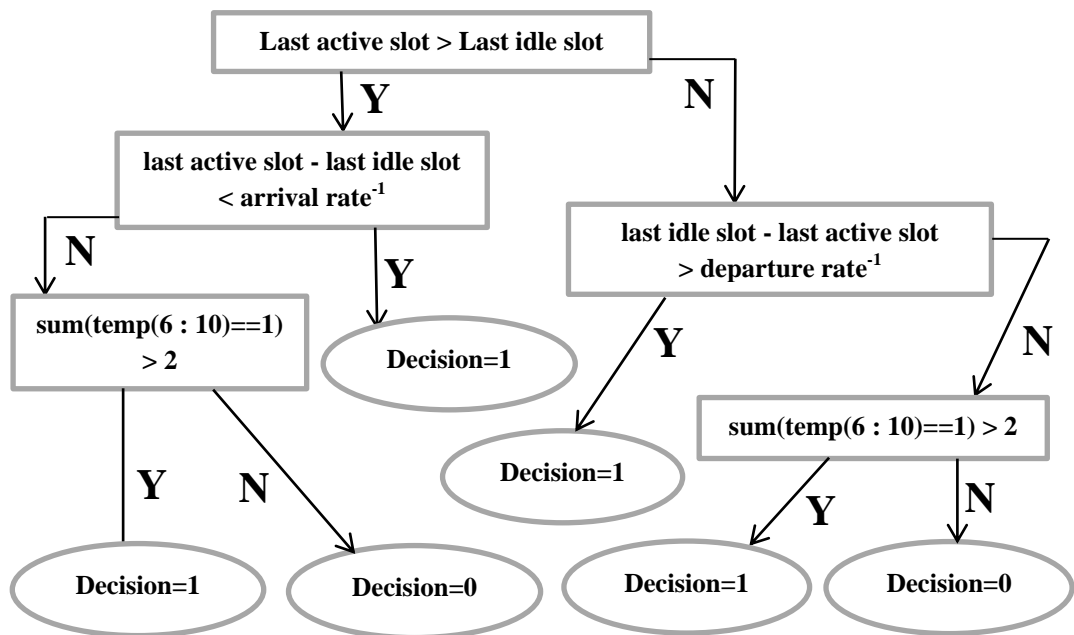


Figure 4.3 Schema of algorithm 2

#### 4.1.1 Binary Estimation Method

In our algorithm collected data from Istanbul Metropolitan Municipality at 10 roads is used. First, it must be converted to binary to be used by the algorithm. Unconverted data consists of raw data of average vehicle speed at single road at certain time interval. Converted data is binary state of average vehicle speed (change between 0-121 km/h) labelled with 0 for above 50 km/h speed and 1 for below 50 km/h.

##### 4.1.1.1 Estimation for Single Road

In this section we have evaluated each road individually and we have estimated density parameter using speed knowledge of that road. For example at D100 Bosphorus Bridge Europe Entry road with route number 60 in 00:00-00:40 time interval, speed data labeled with 0 and 1, then density parameter at time 00:50 has been estimated as 1 or 0. History window length  $W_h$  is 5 and estimation window length  $W_p$  is 1. After the estimation of density at time 00:50, density at time 01:00 is estimated by shifting history window one slot and the process has been repeated. So all data has been scanned, after that, density state of road in all time have been estimated. When free-flow road condition, data 0 is considered as positive, congested road condition data 1 is considered as negative in performance evaluation in Algorithm 1. Because of this, the rate of correct decision of zero is true positive and the rate of correct decision of one is true negative. The rate of all correct decision of all binary data is named as total accuracy. As estimated data has been compared with real binary data, performance analysis can be made as shown in Table 4.1.

Table 4.1 Binary estimation results of algorithm 1 for single road

Rtms Place	Rtms ID	True Positive	True Negative	Total Accuracy
D100 Boğaziçi Köp. Avrupa Gir.	60	0.9375	0.9487	<b>0.9437</b>

Table 4.1 Binary estimation results of algorithm 1 for single road (continue)

Perpa	297	0.9874	0.9126	<b>0.9780</b>
D100 Haliç Köprü Girişi	299	0.9700	0.8125	<b>0.9483</b>
Boğaziçi Köprüsü Yıldız Katılımı	303	0.9616	0.9679	<b>0.9650</b>
D100 Mecidiyeköy B. Köprü Katılımı	305	0.9482	0.9281	<b>0.9398</b>
D100 Çağlayan	363	0.9776	0.9325	<b>0.9664</b>
Okmeydanı Köprüsü	528	0.9912	0.8949	<b>0.9838</b>
Çağlayan SSK	529	0.9870	0.9219	<b>0.9777</b>
Zincirlikuyu İETT Durağı (Tabela)	530	0.9600	0.9479	<b>0.9547</b>
Haliç Köprüsü	267	0.9626	0.8648	<b>0.9414</b>

#### 4.1.1.2 Estimation for Adjacent Roads

In this section, as we have used past speed knowledge of first two roads of three adjacent roads, we have estimated density state of the third road. For example at Okmeydanı Bridge road with route number 528 and Perpa road with route number 297 in 00:00-00:40 time interval, speed data labeled with 0 and 1, then density parameter at Çağlayan SSK with route number 529 at time 00:50 has been estimated as 1 or 0. History window length  $W_h$  is 10 and estimation window length  $W_p$  is 1. After speed data of 528 and 297 numbered roads have been lined up by two different sequences, Algorithm 1 has been run. In the first sequence, first speed data (at time 00:00 in our example) belongs to 528 numbered road and second speed data belongs to 297 numbered road. In brief, last speed data in history window (at time 00:40 in our example) belongs to 297 numbered road. In the second sequence, first five speed data (in 00:00-00:40 time interval in our example) belongs to 528 numbered road and second five speed data belongs to 297 numbered road. All data has been scanned, after then, density state of road in all time have been estimated. Finally, estimated data has been compared with real binary data and performance analysis is concluded. With Algorithm 2, all true positive ratios are decreased a little but we have observed that all true negative ratios and most of total accuracy values are increased as shown in Table 4.2.



Table 4.2 Binary estimation results of algorithms 1 and 2 for adjacent roads

Rtms Place	Rtms ID	Data Seq.	True Positive	True Negative	Total Accuracy	Algorithm
Okmeyd.Köp.Per pa-Çağl. SSK	528-297-529	One	0.9808	0.7472	<b>0.9484</b>	1
Okmeyd.Köp.Per pa-Çağl. SSK	528-297-529	One	0.9796	0.7918	<b>0.9536</b>	2
Okmeyd.Köp.Per pa-Çağl. SSK	528-297-529	Five	0.9910	0.7770	<b>0.9613</b>	1
Okmeyd.Köp.Per pa-Çağl. SSK	528-297-529	Five	0.9766	0.8104	<b>0.9536</b>	2
Okmeyd.Köp.Per pa-Çağl. SSK	297-529-363	One	0.9864	0.5364	<b>0.8807</b>	1
Okmeyd.Köp.Per pa-Çağl. SSK	297-529-363	One	0.9851	0.5806	<b>0.8900</b>	2
Okmeyd.Köp.Per pa-Çağl. SSK	297-529-363	Five	0.9932	0.5430	<b>0.8874</b>	1
Okmeyd.Köp.Per pa-Çağl. SSK	297-529-363	Five	0.9885	0.6026	<b>0.8978</b>	2

#### 4.1.2 Ternary Estimation Method

Converted data is the ternary state of average vehicle speed (change between 0-121 km/h) labelled with 0 if speed value is above 50 km/h (*free-flow*). It is labelled with 1 if speed value is between 50 km/h-30 km/h (*less congested*). If the speed value is below 30 km (*high congested*), it is labelled with 2. In this algorithm the rate of correct decision of zero is zero positive rate, the rate of correct decision of one is one positive rate and the rate of correct decision of two is two positive rate. The rate of all correct decision of all ternary case is named as total accuracy.

##### 4.1.2.1 Estimation for Single Road

In Algorithm 1, one positive rate and two positive rate in road numbers 60, 303, 305 and 530 are very low and because of this, total accuracy values of those roads are not as high as desired. In Algorithm 2, if there are at least three identical values

among last five data, our decision is that ternary value. As estimated data have been compared with real ternary data, we have observed that one positive ratios are slightly increased, two positive ratios and total accuracy values are noticeably increased although zero positive ratios are slightly decreased as shown in Table 4.3.

Table 4.3 Ternary estimation results of algorithms 1 and 2 for single road

<b>Rtms Place</b>	<b>Rtms ID</b>	<b>Zero Positive</b>	<b>One Positive</b>	<b>Two Positive</b>	<b>Total Accuracy</b>	<b>Algorithm</b>
D100 Boğaziçi Köp. Avrupa Girişi	60	0.9665	0.3986	0.3923	<b>0.6534</b>	1
D100 Boğaziçi Köp. Avrupa Girişi	60	0.9375	0.8158	0.5315	<b>0.8362</b>	2
Perpa	297	0.9915	0.1714	0.2300	<b>0.8950</b>	1
Perpa	297	0.9874	0.1714	0.9220	<b>0.9710</b>	2
D100 Haliç Köprü Gir.	299	0.9759	0.5041	0.4619	<b>0.9093</b>	1
D100 Haliç Köprü Gir.	299	0.9700	0.6480	0.5953	<b>0.9238</b>	2
Boğaziçi Köprüsü Yıldız Katılımı	303	0.9730	0.1235	0.1397	<b>0.5179</b>	1
Boğaziçi Köprüsü Yıldız Katılımı	303	0.9616	0.1235	0.9576	<b>0.9376</b>	2
D100 Mecidiyeköy B. Köprü Katılımı	305	0.9590	0.3008	0.2190	<b>0.6534</b>	1
D100 Mecidiyeköy B. Köprü Katılımı	305	0.9482	0.3087	0.9167	<b>0.9025</b>	2
D100 Çağlayan	363	0.9856	0.1687	0.2096	<b>0.7917</b>	1
D100 Çağlayan	363	0.9776	0.2088	0.9302	<b>0.9522</b>	2
Okmeydanı Köprüsü	528	0.9938	0.1977	0.2760	<b>0.9381</b>	1
Okmeydanı Köprüsü	528	0.9912	0.1977	0.9084	<b>0.9796</b>	2
Çağlayan SSK	529	0.9911	0.3029	0.2475	<b>0.8859</b>	1
Çağlayan SSK	529	0.9870	0.3320	0.9200	<b>0.9657</b>	2
Zincir. İETT Dur. Tabela	530	0.9700	0.3850	0.2494	<b>0.6671</b>	1

Table 4.3 Ternary estimation results of algorithms 1 and 2 for single road (continue)

Zincir. İETT Dur. Tabela	530	0.9600	0.4456	0.9121	<b>0.9043</b>	2
Haliç Köprüsü	267	0.9673	0.4009	0.3794	<b>0.8414</b>	1
Haliç Köprüsü	267	0.9626	0.4222	0.7859	<b>0.8981</b>	2

#### 4.1.2.2 Estimation for Adjacent Roads

In Algorithm 1, one positive rate and two positive rate are very low. So we have run Algorithm 2. As estimated data have been compared with real ternary data, we have observed that one positive ratios remained the same, two positive ratios are noticeably increased and zero positive ratios are slightly increased. All of them are causing noticeable increase in total accuracy values as shown in Table 4.4.

Table 4.4 Ternary estimation results of algorithms 1 and 2 for adjacent roads

Rtms Place	Rtms ID	Data Seq.	Zero Positive	One Positive	Two Positive	Total Accuracy	Algorithm
Okmey. Köp.-Perpa-Çağlayan SSK	528-297-529	One	0.9850	0.1026	0.3870	<b>0.8963</b>	1
Okmey. Köp.-Perpa-Çağlayan SSK	528-297-529	One	0.9910	0.1026	0.7957	<b>0.9499</b>	2
Okmey. Köp.-Perpa-Çağlayan SSK	528-297-529	Five	0.9916	0.1026	0.4174	<b>0.9056</b>	1
Okmeyd. Köp.-Perpa-Çağlayan SSK	528-297-529	Five	0.9910	0.1026	0.7957	<b>0.9499</b>	2
Perpa-Çağlayan SSK-D100 Çağlayan	297-529-363	One	0.9871	0.1290	0.2014	<b>0.8013</b>	1
Perpa-Çağlayan SSK-D100 Çağlayan	297-529-363	One	0.9932	0.1290	0.5261	<b>0.8771</b>	2
Perpa-Çağlayan SSK-D100 Çağlayan	297-529-363	Five	0.9932	0.1290	0.1991	<b>0.8055</b>	1
Perpa-Çağlayan SSK-D100 Çağlayan	297-529-363	Five	0.9932	0.1290	0.5261	<b>0.8771</b>	2

## 4.2 Algorithms 3 and 4 Based on Second Method

Second method offered in this study using Markov Chain is depended ON/OFF transition probabilities. We will examine (Black et al., 2012) because of similarities with our methods.

The CR system is considered to be a secondary user (SU) sharing a section of the spectrum allocated to one or more PUs. The purpose of the SU is to increase spectral efficiency by operating in the spectrum holes left by the PU. However, the SU needs not to reduce the PU's quality of service below a predefined level. The spectrum is separated into  $N$  channels each of which has at most one PU in operation.

The CR perceives the state of the spectrum periodically and it is considered that the CR always perceives all channels correctly. Let  $t_i$  (where  $i=0,1,2,\dots$ ) indicate the sensing periods. At each instant  $t_i$  the state of the  $n^{\text{th}}$  channel  $S_n$  is assumed to be either busy or idle,  $S_n(t_i) \in \{\text{BUSY}, \text{IDLE}\}$ . The CR establishes the state comparing the measured energy in channel  $n$  with a threshold value  $p$ . Thus;

$$S_n(t_i) = \begin{cases} 1, & \text{if } e_n(t_i) \geq p \\ 0, & \text{if } e_n(t_i) \leq p \end{cases} \quad (4.7)$$

where:  $e_n(t_i)$  is the energy measured in channel  $n$  at time instant  $t_i$ . If  $S_n(t_i)$  is equal to 1 then the spectrum is busy from time  $t_i$  to  $t_{i+1}$ .

After that, the sequence of states using a Discrete-time Hidden Markov Model (DHMM) can be modeled. This model permits us to make estimations about the location and duration of spectrum holes (Black et al., 2012).

The sequence of spectrum states can be modeled by using a two-state Markov chain with the spectrum in either state  $S_n(t_i) = 1$  or  $S_n(t_i) = 0$ . A Markov chain's property indicates that the probability of future states is dependent on only the past  $m$  states where  $m$  is the order of the Markov chain,

$$P(X_n = x_n / X_{n-1} = x_{n-1}, \dots, X_0 = x_0) = P(X_n = x_n / X_{n-1} = x_{n-1}, \dots, X_{n-m} = x_{n-m}) \quad (4.8)$$

A DHMM occurs from a  $N \times N$  state transmission matrix  $P$  and a  $N \times M$  emission matrix  $Q$  where  $N$  is the number of possible states and  $M$  is the number of possible

emission symbols. If the model has two states, the state transmission matrix is shown as:

$$P = \begin{bmatrix} p_{00} & p_{01} \\ p_{10} & p_{11} \end{bmatrix} \quad (4.9)$$

and if CR is defined as having perfect sensing, the emission matrix will be the identity matrix.

$$Q = \begin{bmatrix} 1 & 0 \\ 0 & 1 \end{bmatrix} \quad (4.10)$$

Figure 4.2 represents the transitions between the states and their probabilities (Black et al., 2012).

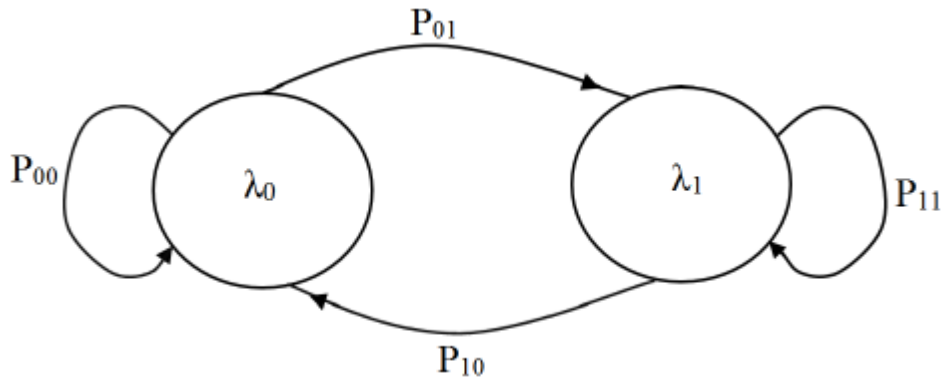


Figure 4.4 A two-state Markov Chain (Black et al., 2012)

The proposed methods in this section use some probability parameters which are obtained by the analysis of decisions in history window. First, state transition probabilities are calculated. After that, decision slot is estimated by comparing these probabilities (Düzenli & Akay, 2015). For Algorithm 3, we calculate these probabilities using Equations (4.11)-(4.16) as shown below.

$$P_0 = \frac{N_0}{|W_H|} \quad (4.11)$$

$$P_1 = \frac{N_1}{|W_H|} \quad (4.12)$$

$$P_{00} = \frac{N_{00}}{N_0} \quad (4.13)$$

$$P_{01} = \frac{N_{01}}{N_0} \quad (4.14)$$

$$P_{10} = \frac{N_{10}}{N_1} \quad (4.15)$$

$$P_{11} = \frac{N_{11}}{N_1} \quad (4.16)$$

where  $P_0, P_1$  are probabilities of being zero and one in history window, respectively.  $P_{00}, P_{01}, P_{10}, P_{11}$  are probabilities of 0-0, 0-1, 1-0, 1-1 transitions in history window, respectively.  $N_0, N_1$  are unconditional probabilities of zero and one in history window, respectively.  $N_{00}, N_{01}, N_{10}, N_{11}$  are numbers of 0-0, 0-1, 1-0, 1-1 transitions in history window, respectively.  $W_H$  is history window length.

We have defined vector cluster which is named temp and used for taking sample at history window length from data in Algorithm 3. Then, we have counted number of 1 and 0 in temp window.

In the second section of Algorithm 3, we have added one to zero-one rate parameter if there is a transition from zero to one and we have calculated other transition like this. After total transitions (1-0, 1-1, 0-1, 0-0) are counted, they are divided by the number of transition state in history window. Therefore, we have calculated probability of transitions ( $P_{00}, P_{01}, P_{10}, P_{11}$ ). Also when we have divided number of 1 and 0 (in ternary estimation additionally 2) to history window length, we have obtained probability of being one ( $P_1$ ) and zero ( $P_0$ ) in history window.

In the third section of Algorithm 3, we have calculated unconditional probability of 0 ( $P(0)$ ) and 1 ( $P(1)$ ) (in ternary estimation additionally 2) by

$$P(0) = (P_{00} * P_0) + (P_{10} * P_1) \quad (4.17)$$

$$P(1) = (P_{01} * P_0) + (P_{11} * P_1) \quad (4.18)$$

Depending on the highest unconditional probability value in binary or ternary case, estimation slot is assigned the corresponding value. If unconditional probability values are equal, estimation slot is assigned as the majority state. Nevertheless if number of transition state in history window are equal, the decision slot will be the last data of history window.

In the fourth section of Algorithm 3, if binary value is 0 and decision slot is 0, we have added one to true positive parameter. If binary value is 1 and decision slot is 1, we have added one to true negative parameter. When we have divided total true positive to total number of 0 and we have divided total true negative to total number of 1, we have found the values of true positive ratio and true negative ratio. Success rate is the addition of total true positive and total true negative. We have computed total accuracy with dividing success to total number of ones and zeros. This method is summarized in **Algorithm 3** below.

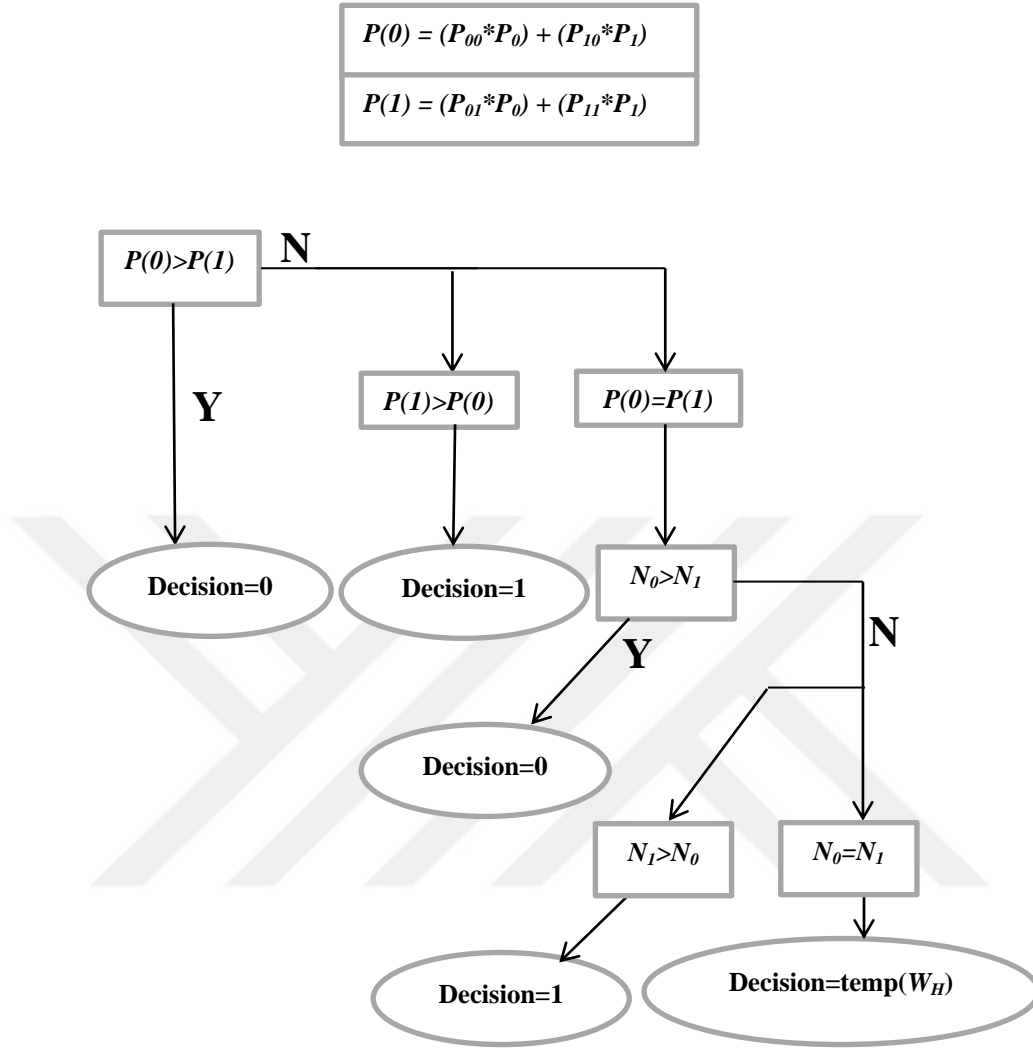


Figure 4.5 Schema of algorithm 3

For Algorithm 4, we calculate the probabilities in Equations (4.19)-(4.26) as shown below

$$P(H_{|W_H|+1} = 0 / H_{|W_H|} = 0) = \frac{N_{00}}{|W_H|-1} \quad (4.19)$$

$$P(H_{|W_H|+1} = 1 / H_{|W_H|} = 0) = \frac{N_{01}}{|W_H|-1} \quad (4.20)$$

$$P(H_{|W_H|+1} = 0 / H_{|W_H|} = 1) = \frac{N_{10}}{|W_H|-1} \quad (4.21)$$



$$P(H_{|W_H|+1} = 1/H_{|W_H|} = 1) = \frac{N_{11}}{|W_H|-1} \quad (4.22)$$

$$\hat{P}_{00} = P(H_{|W_H|+1} = 0/H_{|W_H|} = 0). P_0 \quad (4.23)$$

$$\hat{P}_{01} = P(H_{|W_H|+1} = 1/H_{|W_H|} = 0). P_0 \quad (4.24)$$

$$\hat{P}_{10} = P(H_{|W_H|+1} = 0/H_{|W_H|} = 1). P_1 \quad (4.25)$$

$$\hat{P}_{11} = P(H_{|W_H|+1} = 1/H_{|W_H|} = 1). P_1 \quad (4.26)$$

where  $P_0, P_1$  are probabilities of being zero and one in history window, respectively.  $\hat{P}_{00}, \hat{P}_{01}, \hat{P}_{10}, \hat{P}_{11}$  are conditional probabilities of 0-0, 0-1, 1-0, 1-1 transitions in history window, respectively.  $N_{00}, N_{01}, N_{10}, N_{11}$  are numbers of 0-0, 0-1, 1-0, 1-1 transitions in history window, respectively.  $W_H$  is history window length.

In the first section of Algorithm 4, we have defined temp history window and then we have counted number of 1 and 0 (in ternary estimation additionally 2) in temp window.

In the second section of Algorithm 4, we have added one to one-zero rate parameter if there is a transition from one to zero and we have calculated other transition similarly. After total transitions are counted, they are divided by history window length minus 1 (all state transition number is equal to history window length minus 1). Also when we have divided number of 1 and 0 (in ternary estimation, additionally 2) by history window length, we have obtained probability of being one and zero in history window. By using Equations (4.23)-(4.26), we have calculated conditional probability of transitions ( $\hat{P}_{00}, \hat{P}_{01}, \hat{P}_{10}, \hat{P}_{11}$ ).

In the third section of Algorithm 4, we have evaluated probability values individually. In which transition probability of binary or ternary state is high, we



#### 4.2.1 Binary Estimation Method

In Algorithms 3 and 4, collected data from Istanbul Metropolitan Municipality of 10 roads are used similarly as in the previous algorithms. First, raw data must be converted into binary form. Unconverted data consists of raw data which is the average vehicle speed at single roadway at certain time interval. Converted data is binary state of average vehicle speed (change between 0-121 km/h) labelled as 0 for speed values above 50 km/h and as 1 for speed values below 50 km/h.

##### 4.2.1.1 Estimation for Single Road

We have observed that all true positive ratios, true negative ratios and total accuracy values of Algorithm 3 are equal with Algorithm 4's as shown in Table 4.5.

Table 4.5 Binary estimation results of algorithms 3 and 4 for single road

Rtms Place	Rtms ID	True Positive	True Negative	Total Accuracy	Algorithm
D100 Boğaziçi Köp. Avrupa Girişi	60	0.9060	0.9419	<b>0.9257</b>	3
D100 Boğaziçi Köp. Avrupa Girişi	60	0.9060	0.9419	<b>0.9257</b>	4
Perpa	297	0.9801	0.8519	<b>0.9639</b>	3
Perpa	297	0.9801	0.8519	<b>0.9639</b>	4
D100 Haliç Köprü Girişi	299	0.9600	0.7430	<b>0.9301</b>	3
D100 Haliç Köprü Girişi	299	0.9600	0.7430	<b>0.9301</b>	4
Boğaziçi Köprüsü Yıldız Katılımı	303	0.9324	0.9457	<b>0.9396</b>	3
Boğaziçi Köprüsü Yıldız Katılımı	303	0.9324	0.9457	<b>0.9396</b>	4
D100 Mecidiyeköy B. Köprü Kat.	305	0.9220	0.8874	<b>0.9075</b>	3
D100 Mecidiyeköy B. Köprü Kat.	305	0.9220	0.8874	<b>0.9075</b>	4
D100 Çağlayan	363	0.9633	0.8803	<b>0.9426</b>	3
D100 Çağlayan	363	0.9633	0.8803	<b>0.9426</b>	4
Okmeydanı Köprüsü	528	0.9873	0.8311	<b>0.9753</b>	3
Okmeydanı Köprüsü	528	0.9873	0.8311	<b>0.9753</b>	4
Çağlayan SSK	529	0.9790	0.8582	<b>0.9618</b>	3
Çağlayan SSK	529	0.9790	0.8582	<b>0.9618</b>	4
Zincirlikuyu İETT Durağı (Tabela)	530	0.9339	0.9134	<b>0.9250</b>	3
Zincirlikuyu İETT Durağı (Tabela)	530	0.9339	0.9134	<b>0.9250</b>	4
Haliç Köprüsü	267	0.9466	0.8181	<b>0.9188</b>	3
Haliç Köprüsü	267	0.9466	0.8181	<b>0.9188</b>	4

#### 4.2.1.2 Estimation for Adjacent Roads

We have observed that although most of true negative ratios of Algorithm 4 are higher than Algorithm 3's, most of true positive ratios of Algorithm 3 are higher than Algorithm 4's and total accuracy values of two algorithms from the point of superiority view are equal as shown in Table 4.6.

Table 4.6 Binary estimation results of algorithms 3 and 4 for adjacent roads

Rtms Place	Rtms ID	Data Seq.	True Positive	True Negative	Total accuracy	Algorithm
Okmeydanı Köprüsü-Perpa-Çağlayan SSK	528-297-529	One	0.9904	0.6171	<b>0.9386</b>	3
Okmeydanı Köprüsü-Perpa-Çağlayan SSK	528-297-529	One	0.9898	0.5948	<b>0.9350</b>	4
Okmeydanı Köprüsü-Perpa-Çağlayan SSK	528-297-529	Five	0.9904	0.6171	<b>0.9386</b>	3
Okmeydanı Köprüsü-Perpa-Çağlayan SSK	528-297-529	Five	0.9904	0.7063	<b>0.9510</b>	4
Perpa-Çağlayan SSK-D100 Çağlayan	297-529-363	One	0.9946	0.5077	<b>0.8802</b>	3
Perpa-Çağlayan SSK-D100 Çağlayan	297-529-363	One	0.9919	0.5077	<b>0.8781</b>	4
Perpa-Çağlayan SSK-D100 Çağlayan	297-529-363	Five	0.9946	0.5077	<b>0.8852</b>	3
Perpa-Çağlayan SSK-D100 Çağlayan	297-529-363	Five	0.9939	0.5386	<b>0.8869</b>	4

#### 4.2.2 Ternary Estimation Method

Collected data from Istanbul Metropolitan Municipality of 10 roads, must be converted to ternary form before used in the algorithms. Converted data is ternary state of average vehicle speed (change between 0-121 km/h) labelled with 0 if speed value is above 50 km/h (*free-flow*). It is labelled with 1 if speed value is between 50 km/h-30 km/h (*less congested*). If speed value is below 30 km/h (*high congested*), it is labelled with 2.

#### 4.2.2.1 Estimation for Single Road

We have observed that although nearly all one positive ratios and all two positive ratios of Algorithm 3 are higher than Algorithm 4's, all zero positive ratios and nearly all total accuracy values of Algorithm 4 are higher than Algorithm 3's as shown in Table 4.7.

Table 4.7 Ternary estimation results of algorithms 3 and 4 for single road

Rtms Place	Rtms ID	Zero Positive	One Positive	Two Positive	Total Accuracy	Algorithm
D100 Boğaziçi Köp. Av. Gir.	60	0.9068	0.8402	0.4654	<b>0.8248</b>	3
D100 Boğaziçi Köp. Av. Gir.	60	0.9365	0.7813	0.4326	<b>0.8090</b>	4
Perpa	297	0.9804	0.1071	0.8575	<b>0.9567</b>	3
Perpa	297	0.9906	0.0857	0.8562	<b>0.9653</b>	4
D100 Haliç Köprü Girişi	299	0.9610	0.5876	0.4597	<b>0.9049</b>	3
D100 Haliç Köprü Girişi	299	0.9731	0.5272	0.4513	<b>0.9090</b>	4
Boğaziçi Köprüsü Yıldız Kat.	303	0.9329	0.0529	0.9432	<b>0.9152</b>	3
Boğaziçi Köprüsü Yıldız Kat.	303	0.9762	0.0471	0.9312	<b>0.9284</b>	4
D100 Mecidiye. B. Köprü Kat.	305	0.9244	0.1858	0.8749	<b>0.8669</b>	3
D100 Mecidiye. B. Köprü Kat.	305	0.9658	0.1701	0.8668	<b>0.8871</b>	4
D100 Çağlayan	363	0.9646	0.1124	0.8813	<b>0.9293</b>	3
D100 Çağlayan	363	0.9857	0.1044	0.8774	<b>0.9441</b>	4
Okmeydanı Köprüsü	528	0.9874	0.0349	0.8515	<b>0.9712</b>	3
Okmeydanı Köprüsü	528	0.9938	0.0698	0.8379	<b>0.9761</b>	4
Çağlayan SSK	529	0.9798	0.1909	0.8648	<b>0.9499</b>	3
Çağlayan SSK	529	0.9917	0.1743	0.8601	<b>0.9592</b>	4
Zincirlikuyu İETT Dur. (Tabela)	530	0.9349	0.3008	0.8788	<b>0.8673</b>	3
Zincirlikuyu İETT Dur. (Tabela)	530	0.9716	0.2752	0.8637	<b>0.8807</b>	4
Haliç Köprüsü	267	0.9495	0.3507	0.7239	<b>0.8737</b>	3
Haliç Köprüsü	267	0.9684	0.2953	0.6932	<b>0.8801</b>	4

#### 4.2.2.2 Estimation for Adjacent Roads

We have observed that although most of one positive ratios of Algorithm 4 are higher than Algorithm 3's, all zero positive ratios and most of total accuracy values

of Algorithm 3 are higher than Algorithm 4's and two positive ratios of two algorithms from the point of superiority view are equal as shown in Table 4.8.

Table 4.8 Ternary estimation results of algorithms 3 and 4 for adjacent roads

<b>Rtms Place</b>	<b>Rtms ID</b>	<b>Data Seq.</b>	<b>Zero Positive</b>	<b>One Positive</b>	<b>Two Positive</b>	<b>Total Accuracy</b>	<b>Algorithm</b>
Okmeyd. Köp.- Perpa-Çağl. SSK	528-297- 529	One	0.9928	0.0256	0.6391	<b>0.9314</b>	3
Okmeyd. Köp.- Perpa-Çağl. SSK	528-297- 529	One	0.9910	0.0513	0.6217	<b>0.9283</b>	4
Okmeyd. Köp.- Perpa-Çağl. SSK	528-297- 529	Five	0.9934	0.0256	0.6522	<b>0.9334</b>	3
Okmeyd. Köp.- Perpa-Çağl. SSK	528-297- 529	Five	0.9928	0.0513	0.7261	<b>0.9422</b>	4
Perpa-Çağl. SSK- D100 Çağlayan	297-529- 363	One	0.9953	0.0968	0.5024	<b>0.8729</b>	3
Perpa-Çağl. SSK- D100 Çağlayan	297-529- 363	One	0.9925	0.0968	0.4763	<b>0.8651</b>	4
Perpa-Çağl. SSK- D100 Çağlayan	297-529- 363	Five	0.9953	0.0968	0.5024	<b>0.8729</b>	3
Perpa-Çağl. SSK- D100 Çağlayan	297-529- 363	Five	0.9946	0.0968	0.5047	<b>0.8729</b>	4

### 4.3 Evaluation of Results

Sample accuracy (acc) is the most frequently used performance criterion of a multiclass classifier which is defined as the number of correct predictions across all classes,  $k$ , divided by the number of examples,  $n$  (Carrillo, Brodersen & Castellanos, 2013).

For overcoming the limitations of sample accuracies, another performance evaluation parameter, the Kappa coefficient, is used in the domain of remote sensing problems (Cohen, 1960). It measures the degree of overall agreement within a given matrix.

$$K_c = \frac{p_o - p_e}{1 - p_e} \quad (4.27)$$

$$p_o = \frac{1}{l} \sum_{i=1}^l k_i, \quad p_e = \frac{1}{l^2} \sum_{i=1}^l C_{i+} \times C_{+i} \quad (4.28)$$

where  $k_i$  is the number of correct predictions in class  $i$  and  $l$  is the number of classes.  $C_{i+}$  and  $C_{+i}$  are the row-wise and column-wise sums of row and column  $i$  in the confusion matrix, respectively.

$K_c$  is calculated for the degree of class instability in the data. However, it can be invariant to the number of misclassifications and does not necessarily express what one would consider prediction strength (Cohen, 1960).

The balanced accuracy  $\hat{\lambda}$  (bac) is an alternative parameter which is defined as the average accuracy obtained on all classes. In the case of a multi-class classification problem, its formula is given by

$$\hat{\lambda} = \frac{1}{l} \sum_{i=1}^l \frac{k_i}{n_i} \quad (4.29)$$

where  $n_i$  is the number of examples in class  $i$ . The balanced accuracy is commonly used in these problems and has several advantages to other criteria because of its simplicity (Nishii & Tanaka, 1999).

We have evaluated our algorithms by these criteria which can be used on performance analysis. We have used true positive, true negative, zero positive, one positive, and two positive parameters in binary and ternary estimation of single road case and adjacent roads case. We have used road 529 Çağlayan SSK as single road, 528-297-529 roads as adjacent roads.

Table 4.9 Binary estimation results of the best algorithms for road 529

Rtms Place	Rtms ID	True Positive	True Negative	Algorithm
Çağlayan SSK	529	0.9870	0.9219	1
Çağlayan SSK	529	0.9790	0.8582	4

Table 4.10 Confusion matrix of binary estimation for road 529 of algorithm 1

	0	1	
0	<b>10222</b>	135	<b>10357</b>
1	135	<b>1593</b>	<b>1728</b>
Total	<b>10357</b>	<b>1728</b>	

Table 4.11 Confusion matrix of binary estimation for road 529 of algorithm 4

	0	1	
0	<b>10140</b>	245	<b>10385</b>
1	217	<b>1483</b>	<b>1700</b>
Total	<b>10357</b>	<b>1728</b>	

Table 4.12 Binary estimation results of the best algorithms for adjacent roads

Rtms Place	Rtms ID	True Positive	True Negative	Algorithm
Okmeydanı Köprüsü-Perpa-Çağlayan SSK	528-297-529	0.9796	0.7918	2
Okmeydanı Köprüsü-Perpa-Çağlayan SSK	528-297-529	0.9904	0.6171	3

Table 4.13 Confusion matrix of binary estimation for adjacent roads of algorithm 2

	0	1	
0	<b>1635</b>	56	<b>1691</b>
1	34	<b>213</b>	<b>247</b>
Total	<b>1669</b>	<b>269</b>	

Table 4.14 Confusion matrix of binary estimation for adjacent roads of algorithm 3

	0	1	
0	<b>1653</b>	103	<b>1756</b>
1	16	<b>166</b>	<b>182</b>
Total	<b>1669</b>	<b>269</b>	



Table 4.15 Comparison of the best binary algorithms

<b>Rtms Place</b>	<b>Rtms ID</b>	<b>acc</b>	<b>bac</b>	<b>Kc</b>	<b>Algorithm</b>
Çağlayan SSK	529	<b>0.9777</b>	<b>0.9544</b>	<b>0.9088</b>	1
Çağlayan SSK	529	<b>0.9618</b>	<b>0.9186</b>	<b>0.8430</b>	4
Okmeydanı Köprüsü- Perpa-Çağlayan SSK	528-297- 529	<b>0.9536</b>	<b>0.8857</b>	<b>0.7989</b>	2
Okmeydanı Köprüsü- Perpa-Çağlayan SSK	528-297- 529	<b>0.9386</b>	<b>0.8038</b>	<b>0.7029</b>	3

Table 4.16 Ternary estimation results of the best algorithms for road 529

<b>Rtms Place</b>	<b>Rtms ID</b>	<b>Zero Positive</b>	<b>One Positive</b>	<b>Two Positive</b>	<b>Algorithm</b>
Çağlayan SSK	529	0.9870	0.3320	0.9200	2
Çağlayan SSK	529	0.9917	0.1743	0.8601	4

Table 4.17 Confusion matrix of ternary estimation for road 529 of algorithm 2

	0	1	2	
0	<b>10222</b>	94	41	<b>10357</b>
1	83	<b>80</b>	78	<b>241</b>
2	52	67	<b>1368</b>	<b>1487</b>
	<b>10357</b>	<b>241</b>	<b>1487</b>	

Table 4.18 Confusion matrix of ternary estimation for road 529 of algorithm 4

	0	1	2	
0	<b>10271</b>	132	193	<b>10596</b>
1	33	<b>42</b>	15	<b>90</b>
2	53	67	<b>1279</b>	<b>1399</b>
	<b>10357</b>	<b>241</b>	<b>1487</b>	

Table 4.19 Ternary estimation results of the best algorithms for adjacent roads

<b>Rtms Place</b>	<b>Rtms ID</b>	<b>Zero Positive</b>	<b>One Positive</b>	<b>Two Positive</b>	<b>Algorithm</b>
Okmeydanı Köprüsü- Perpa-Çağlayan SSK	528-297- 529	0.9910	0.1026	0.7957	2
Okmeydanı Köprüsü- Perpa-Çağlayan SSK	528-297- 529	0.9928	0.0256	0.6391	3

Table 4.20 Confusion matrix of ternary estimation for adjacent roads of algorithm 2

	0	1	2	
0	<b>1654</b>	23	35	<b>1712</b>
1	7	<b>4</b>	12	<b>23</b>
2	8	12	<b>183</b>	<b>203</b>
	<b>1669</b>	<b>39</b>	<b>230</b>	

Table 4.21 Confusion matrix of ternary estimation for adjacent roads of algorithm 3

	0	1	2	
0	<b>1657</b>	30	81	<b>1768</b>
1	0	<b>1</b>	2	<b>3</b>
2	12	8	<b>147</b>	<b>167</b>
	<b>1669</b>	<b>39</b>	<b>230</b>	

Table 4.22 Comparison of the best ternary algorithms

Rtms Place	Rtms ID	acc	bac	Kc	Algorithm
Çağlayan SSK	529	<b>0.9657</b>	<b>0.7463</b>	<b>0.8626</b>	2
Çağlayan SSK	529	<b>0.9592</b>	<b>0.6754</b>	<b>0.8258</b>	4
Okmey. Köp.-Perpa-Çağlayan SSK	528-297-529	<b>0.9499</b>	<b>0.6297</b>	<b>0.7791</b>	2
Okmey. Köp.-Perpa-Çağlayan SSK	528-297-529	<b>0.9314</b>	<b>0.5525</b>	<b>0.6637</b>	3

In cognitive radio application, two performance criteria are generally used. These are introduced below.

**System Utility:** This criterion shows the rate of correct decision of spectrum hole slots. It is related to **true positive ratio** in our algorithms.

**Primary User Disturbance Ratio:** This criterion shows the rate of false decision of active PU slots. It is related to **false negative ratio** in our algorithms.

Desired situation is True Positive Ratio=1 and False Negative Ratio=0.

Table 4.23 Comparison of the algorithm 1 and other prediction methods

<b>Rtms ID</b>	<b>True Positive</b>	<b>False Negative</b>	<b>Total Accuracy</b>	<b>Best Algorithms</b>
529	<b>0.9870</b>	<b>0.0781</b>	<b>0.9777</b>	Algorithm 1
529	<b>0.9863</b>	<b>0.0799</b>	<b>0.9768</b>	Correlation
529	<b>0.9863</b>	<b>0.0799</b>	<b>0.9768</b>	Linear regression
529	<b>0.9609</b>	<b>0.2477</b>	<b>0.9311</b>	Auto-correlation

We can see that our algorithm is more succesful than other prediction methods used in cognitive radio applications like Correlation, Lineer regression and Auto-correlation in all performance criteria.



## CHAPTER FIVE

### CONCLUSION

In this thesis, as alternative to the methods used in the literature, new and simplified density estimation algorithms have been proposed. These algorithms are inspired by the methods used to estimate spectrum holes in cognitive radio channels. We have attempted to estimate the density of traffic with the same approach. All proposed algorithms estimate the next state of the road by looking at only the history of density data. Because of simplicity of our proposed algorithms, they can be preferred to the other density estimation methods. The other advantages of proposed algorithms are using only past density data as traffic parameters and high success rate.

In this study, Istanbul Metropolitan Municipality Traffic Control Center data gathered from the busiest roads of Istanbul in 2013, have been used as traffic data. The raw data have been converted into binary and ternary form and defective measurements are removed before application. The algorithms using converted data have been tested by simulating two different scenarios. In the first scenario, the algorithms have estimated traffic state in the 60<sup>th</sup> minute of the road by looking at past 50 minutes of density data of the same road. In the second scenario, the algorithms have estimated traffic state in the 60<sup>th</sup> minute of the third adjacent road by looking at past 50 minutes of density data of the preceding roads.

By evaluating estimation results with three different performance criteria, we have determined which algorithms are better at which estimation scenarios. When we have considered results separately as binary and ternary, we have expected that binary estimation's performance to be higher. Because we have made a more general acceptance with one threshold in binary estimation. When we compare all of the results, we observed that Algorithm 1 is the best at binary estimation at road 529 named Çağlayan SSK, Algorithm 2 is the best at binary estimation of adjacent roads and ternary estimation of both road 529 and adjacent roads case.

We have also observed that ternary estimation of proposed algorithms have very low one positive rate. When we have examined the results exhaustively, we observed that the errors are due to sudden changes in the density data. These sudden changes are probably caused by unexpected incidents, such as seasonal factors like rain, snow etc. and traffic accidents.

But why these events may have influenced severely one positive rates in the ternary estimation? In our study, we saw that the less congested (ternary 1 state) traffic state in the ternary estimation case is the transition state having low probability of being in ternary data compared to the other two states. Additionally, an unexpected traffic incident is an event which changes traffic state suddenly and affects the traffic in the long run. For example, when state of a road is free-flow (ternary 0 state) and a traffic accident suddenly occurs, the state of the road will be high congested (ternary 2 state) at that moment. But we have observed that the probability of coincidence of this transition (from 0 to 2 transition) moments and estimated moment (estimated slot in algorithms) is very low. Therefore, the effect of these errors on two positive rate is less. On the other hand, proposed algorithms can not estimate correctly the state in which traffic is high congested in long term by effects of the incident and then when these effects disappear it is passing to less congested case. Because, if past ten states are high congested (ten slots are 2 in history window) naturally, algorithms estimate the state of the road as high congested (estimated slot is 2). We have observed that the probability of coincidence of this transition (from 2 to 1 transition) moments and estimated moment (estimated slot) is high and the possibility of less congested (ternary 1 state) traffic state being in ternary data is low. Therefore, one positive rate fall down seriously in ternary estimation. Although these events impact binary estimations as well, total accuracy values of binary estimations are very high due to the fact that the number of transitions of 0 state to 1 state (and from 1 to 0) at estimated moments are low and probabilities of 0 and 1 states being in binary data are close and relatively high.

For solving this problem in future studies, by making unexpected traffic events as an additional system parameter in the algorithms, it is planned to increase the success

rate. Also neural networks can be used to create a model for a specific road with the help of history data. Accurate modeling of a road segment will improve the accuracy of estimation of future traffic density.



## REFERENCES

- Alvarez-Icaza, L., Munoz, L., Sun, X., & Horowitz, R. (2004). Adaptive observer for traffic density estimation. *Proceeding of the 2004 American Control Conference*, 2705-2710. Boston, Massachusetts.
- Black, T., Kerans, B., & Kerans, A. (2012). Implementation of hidden Markov model spectrum prediction algorithm. *International Symposium on Communications and Information Technologies (ISCIT)*, 280-283, Gold Coast, QLD.
- Canberk, B., Akyildiz, I. F., & Oktug, S. (2011). Primary user activity modeling using first- difference filter clustering and correlation in cognitive radio networks. *IEEE/ACM Transactions on Networking*, 19 (1), 170-183.
- Carrillo, H., Brodersen, K. H., & Castellanos, J. H. (2013). Probabilistic performance evaluation for multiclass classification using the posterior balanced accuracy. *ROBOT2013: First Iberian Robotics Conference*, 347-361.
- Chu, L., Oh, J.-S., & Recker, W. (2005). Adaptive Kalman filter based freeway travel time estimation. *Transportation Research Board 84th Annual Meeting, CD-ROM*, 1118.
- Chun-Hao, L., Gabran, W., & Cabric, D. (2012). Prediction of exponentially distributed primary user traffic for dynamic spectrum access. *IEEE Global Communications Conference (GLOBECOM)*, 1441-1446, Anaheim, CA.
- Cohen, J. (1960). A coefficient of agreement for nominal scales. *Educational and Psychological Measurement*, 20 (1), 37-46.
- Daganzo, C. F. (1995a). A finite difference approximation of the kinematic wave model of traffic flow. *Transportation Research Part B:Methodological*, 29 (4), 261-276.

- Daganzo, C. F. (1995b). The cell transmission model, part II: network traffic. *Transportation Research Part B:Methodological*, 29 (2), 79-93.
- Düzenli, T. (2015). *Prediction of primary user state in cognitive radios in the presence of time varying arrival rates*. 3rd P.hD. Thesis Progression Report, İzmir: Electrical and Electronics Engineering Department, Dokuz Eylül University.
- Düzenli, T., & Akay, O. (2015). Channel state prediction for cognitive radios with stochastically varying primary user traffic density. *23th Signal Processing and Communications Applications Conference (SIU)*, 1232-1235, Malatya, Turkey.
- Kalman, R., (1960). A new approach to linear filtering and prediction problems. *Journal of Basic Engineering*, 82 (1), 35-45.
- Kay, S. (2006). *Intuitive probability and random processes using matlab*. New York, USA: Springer.
- Kim, H., & Shin, K. (2008). Efficient discovery of spectrum oppurtunities with mac-layer sensing in cognitive radio networks. *IEEE Transactions Mobile Computing*, 7 (5), 545-553.
- Lighthill, M. J., & Whitham, G. B. (1955). On kinematic waves II: a theory of traffic flow on long crowded roads. *Proceedings of the Royal Society of London, Series A Mathematical and Physical Sciences*, 229 (1178), 317-345.
- Lopez-Benitez, M., & Casadevall, F. (2011). Discrete-time spectrum occupancy model based on Markov chain and duty cycle models. *Proc. of the IEEE Symposia on New Frontiers in Dynamic Spectrum Access Networks (DySPAN)*, 90-99.



- Munoz, L., Sun, X., Horowitz, R., & Alvarez, L. (2003). Traffic density estimation with the cell transmission model. *Proceedings of the American Control Conference*, 3750-3755, Denver, Colorado.
- Nishii, R., & Tanaka, S., (1999). Accuracy and inaccuracy assessments in land-cover classification. *Geoscience and Remote Sensing, IEEE Transactions on*, 37 (1), 491-498.
- Qiu, Z. (2007). *Macroscopic traffic state estimation for large scale freeway network using wireless network data*. P.hD. Thesis, University of Wisconsin-Madison, Wisconsin.
- Richards, P. I. (1956). Shock waves on the highway. *Operations Research*, 4 (1), 42-51.
- Rodgers J. L., & Nicewander, A. W. (1988). Thirteen ways to look at the correlation coefficient. *American Statistician*, 42 (1), 59-66.
- Roess, R. P., Prassas, E. S., & McShane, W. R. (2004). *Traffic engineering*. New Jersey, USA: Pearson Education International.
- Sun, X. (2005). *Modeling, estimation, and control of freeway traffic*. P.hD. Thesis, University of California, Berkeley, California.
- Uyanık, G. S., Canberk, B., & Oktuğ, S. (2012). Predictive spectrum decision mechanisms in cognitive radio networks. *IEEE Globecom Workshops (GC Wkshps)*, 943-947, Anaheim, CA.
- Wilkomm, D., Machiraju, S., Bolot, J., & Wolisz, A. (2008). Primary users in cellular networks: a large-scale measurement study. *Proc. of the IEEE Symposia on New Frontiers in Dynamic Spectrum Access Networks (DySPAN)*, 1-11.

Yang, L. (2012). *Stochastic traffic flow modeling and optimal congestion pricing*. P.hD. Thesis, The University of Michigan, Michigan.

Ye, Z. (2007). *Speed estimation using single loop detector outputs*. P.hD. Thesis, Texas A&M University, Texas.

